ELSEVIER

ICARUS
International Journal of Solar System Studies

Detailed infrared study of amorphous to crystalline propionitrile ices relevant to observed spectra of Titan's stratospheric ice clouds

Check for updates

Delphine Nna-Mvondo[a,b,*], C.M. Anderson[a], R.E. Samuelson[a,c]

[a] *NASA Goddard Space Flight Center, Greenbelt, MD, USA*
[b] *Universities Space Research Association (USRA), Columbia, MD, USA*
[c] *University of Maryland, College Park, MD, USA*

ABSTRACT

We have conducted a comprehensive study of propionitrile (C_2H_5CN) ice from the amorphous to crystalline phase in order to provide detailed information on this specific cyanide, which may potentially contribute to the chemical composition of the Haystack ice cloud observed in Titan's stratosphere by the Cassini Composite InfraRed Spectrometer (CIRS). Infrared transmission spectra of thin films of pure propionitrile ices deposited at low temperature (30–160 K) were collected from $50\,cm^{-1}$ to $11{,}700\,cm^{-1}$ (200–0.85 μm). The far-infrared spectral region was specifically targeted to compare with CIRS far-infrared limb spectra. The temperature and time evolution of C_2H_5CN ice was thoroughly investigated to better understand discrepancies reported in previously published laboratory studies on the crystalline phase of C_2H_5CN. Specifically, we observe peculiar temperature and time-driven ice phase transitions, revealed by significant spectral variations in the ice, which stabilizes once a complete crystalline phase is achieved. From these results, the crystalline phase of propionitrile ice was identified at deposition temperatures greater than or equal to 135 K and < 140 K. Our findings corroborate previous studies that ruled out pure propionitrile ice as the sole chemical identity of Titan's observed Haystack emission feature. In order to understand and identify the Haystack cloud, we have initiated co-deposition experiments that incorporate mixtures of Titan-relevant organics, many of which have corresponding vapors that are abundantly present in Titan's stratosphere. In this paper, we present the result of one example of a co-deposited ternary ice mixture containing 16% hydrogen cyanide (HCN), 23% C_2H_5CN, and 61% benzene (C_6H_6). Although this co-condensed ice mixture is the best fit thus far obtained to match the broad width of the Haystack, it is still not the appropriate chemical candidate. However, it reveals an intriguing result: the strong lattice mode of pure C_2H_5CN ice is drastically altered by the surrounding molecules as a result of mixing in a co-condensed phase. The laboratory results reported here on propionitrile ice may help to further constrain the chemical identification of Titan's stratospheric Haystack ice cloud, as well as improve on the current state of knowledge of Titan's stratospheric ice cloud chemistry.

1. Introduction

Propionitrile (C_2H_5CN), also known as ethyl cyanide or propanenitrile, is an aliphatic saturated mononitrile, proposed to form in Titan's atmosphere in the vapor phase from two different neutral-neutral reactions: (1) the combination of the excited-state of the nitrogen atom N (^2D) with propene (C_3H_6) in a similar formation pathway as that of acetonitrile (CH_3CN) (Krasnopolsky, 2009; Vuitton et al., 2007), and (2) the direct reaction of the CH_2CN radical with the CH_3 radical (Loison et al., 2015). Likewise, laboratory simulations of Titan's atmospheric chemistry have also been predicting the production of gaseous C_2H_5CN in Titan's atmosphere for nearly two decades (Coll et al., 1999;

Fujii and Arai, 1999; Thompson et al., 1991). However, it was not until early in the Cassini mission when in-situ measurements made by the Ion and Neutral Mass spectrometer (INMS) were used to infer the presence of gaseous C_2H_5CN in Titan's upper atmosphere at altitudes > 500 km, with a derived mole fraction of 5.0×10^{-7} at 1100 km, 74°N (Vuitton et al., 2007; Vuitton et al., 2006). Vuitton et al. (2006) postulated that protonation of C_2H_5CN may produce the molecular ion $C_2H_5CNH^+$, in which they attributed the April 2005 INMS detection of the mass-to-charge ratio of 56 (Waite et al., 2005; Cravens et al., 2006) to that of $C_2H_5CNH^+$. Shortly afterwards, Magee et al. (2009) analyzed the INMS-measured ion masses between 50 and 56 and determined a C_2H_5CN mixing ratio of 1.54×10^{-7} at 1050 km, which is roughly a

factor of three less than that inferred by Vuitton et al. (2006). Later on, Atacama Large Millimeter/Submillimeter Array (ALMA) ground-based observations were used to estimate trace amounts of C_2H_5CN vapor in Titan's stratosphere, with abundances about 200 to 600 times smaller than those previously derived from Cassini INMS measurements (Cordiner et al., 2015). Specifically, Cordiner et al. (2015) determined gaseous C_2H_5CN mixing ratio estimates of 1.30×10^{-9} at an altitude of 292 km, 3.24×10^{-9} at 200 km, and 0.79×10^{-9} at 100 km. These derived mixing ratios are similar to those previously reported by Marten et al. (2002), in which ground-based measurements using the IRAM 30-m telescope were used to estimate a C_2H_5CN mixing ratio upper limit of 2.0×10^{-9} at an altitude of 300 km. Cassini Composite InfraRed Spectrometer (CIRS) disk-viewing (emission angles < 60°) far-infrared spectra were then utilized by de Kok et al. (2008) to estimate a C_2H_5CN gas mixing ratio upper limit of 8×10^{-9} at latitudes poleward of 70°N in Titan's late northern winter season. More recently, the 1D photochemical model of Loison et al. (2015) estimated higher mole fractions of gaseous propionitrile in Titan's stratosphere, with mixing ratios more similar to those deduced by INMS, and derived a lower mole fraction of $\sim 3 \times 10^{-7}$ around 200 km and a larger value of $\sim 7 \times 10^{-7}$ near 100 km; they also predicted a C_2H_5CN gas enrichment in Titan's polar regions. However, a lower abundance of C_2H_5CN gas is expected in Titan's lower stratosphere compared to that at higher altitudes, assuming a formation scenario consistent with the production of gaseous propionitrile in Titan's upper atmosphere, which will diffuse to lower altitudes, with atmospheric loss resulting from condensation and chemistry in Titan's lower stratosphere (Sagan and Thompson, 1984).

Even though C_2H_5CN gas is expected to condense in Titan's lower stratosphere, as is the case for many other nitriles, i.e. HCN, cyanoacetylene HC_3N, cyanogen C_2N_2 (Sagan and Reid Thompson, 1984; Frère et al., 1990; Raulin and Owen, 2002; Anderson et al., 2016, 2018b), C_2H_5CN ice has never been detected by Cassini CIRS or the Visible and Infrared Mapping Spectrometer (VIMS) at any time over Cassini's 13 year mission. Yet, its presence as a chemical component of one of Titan's observed stratospheric ice clouds has been debated over the last four decades. This debate started after the Voyager 1 flyby of Titan in 1980, when the Infrared Interferometer Spectrometer and Radiometer (IRIS) recorded thermal infrared (IR) spectra of Titan's north polar hood near 70°N, and discovered an intense broad emission feature centered at 221 cm^{-1} in the lower stratosphere near an altitude of 121 km (Samuelson, 1985). Spanning both Voyager and Cassini epochs, this chemically unidentified 221 cm^{-1} emission feature has been referred to by names such as Titan's 220 cm^{-1} feature (Samuelson, 1985, 1992), the 200–240 cm^{-1} feature (Samuelson et al., 1997), unidentified feature 2 (Coustenis et al., 1999), Haze B (de Kok et al., 2007), the far-infrared 220 cm^{-1} cloud (Jennings et al., 2012a), the far-infrared haze (Jennings et al., 2012b), the polar condensate cloud (Jennings et al., 2015), and the Haystack (Anderson et al., 2014). Hereafter, we refer to Titan's 221 cm^{-1} stratospheric ice emission feature as the Haystack. The Haystack was initially thought to form via vapor condensation processes, and was expected to contain a single pure condensed chemical compound. Initially, the Haystack was thought to be comprised of water (H_2O) ice due to the very strong spectral feature of H_2O ice located near 221 cm^{-1} (Samuelson, 1985). Subsequent laboratory transmission spectra of H_2O ice between 70 and 150 K, in both the amorphous and crystalline phase, do not spectrally match the shape of the Haystack ice emission feature; and consequently, H_2O ice was ruled out early on as a candidate for the Haystack (Samuelson, 1992; Coustenis et al., 1999; Samuelson et al., 2007).

The next proposed chemical candidate for the Haystack was C_2H_5CN ice due to its C–C ≡ N (ν_{13}) bending mode near 221 cm^{-1}. Dello Russo and Khanna (1996) were the first investigators to initiate a detailed laboratory study focusing on C_2H_5CN ice related to Titan's observed stratospheric ice clouds. They performed thin ice film transmission spectroscopy and reported spectra and optical constants for crystalline C_2H_5CN ice at 35 K and 95 K. In their study, the crystalline phase of

propionitrile was achieved by depositing the vapor at low temperature (between 50 and 100 K; the exact temperature is not documented), and then warmed to 140 K and annealed for 30–180 min (the exact annealing time duration is not given); and finally, they cooled the annealed sample to 95 K then to 35 K to record its IR spectrum at both temperatures. The investigators reported that the laboratory spectra of annealed crystalline C_2H_5CN ice exhibited a strong absorption band (ν_{13} C-C ≡ N bending mode) at 226 cm^{-1} at 35 K and at 225 cm^{-1} at 95 K, which was spectrally shifted by 5 to 4 cm^{-1}, respectively, to higher energies than that of the IRIS-observed Haystack feature. As a result, C_2H_5CN ice was ruled out as a possible candidate for the Haystack emission feature. Dello Russo and Khanna (1996) also pointed out that the wavenumber position of the C_2H_5CN lattice band was significantly dependent on temperature. In fact, nine years later, Khanna (2005a) reexamined the Dello Russo and Khanna (1996) results, and reported a short laboratory work exclusively focused on crystalline propionitrile. Khanna (2005a) reassessed the laboratory IR spectra of crystalline propionitrile by varying the annealing temperature and duration, considering that in the previous analysis by Dello Russo and Khanna (1996), they were unsuccessful in attaining the most stable crystalline phase of C_2H_5CN. Khanna (2005a) obtained a new crystalline sample after depositing the vapor at 60 K, then annealing at 120 K for 4 h (and then cooled back down to various temperatures, as low as 15 K), which revealed the ν_{13} band peaking at 221 cm^{-1}. Even though this result contradicted the previous results from the Dello Russo and Khanna (1996) study, Khanna (2005a) concluded that condensed C_2H_5CN is the predominant contributor to Titan's Haystack emission feature, with minor contribution from both HC_3N and H_2O ices. Khanna (2005a) also noted additional spectral discrepancies from their earlier work for other C_2H_5CN bands (i.e. at 547 cm^{-1} and at 780 cm^{-1}), which could result from temperature dependences that may alter the peak positions and widths of these two bands. However, no further study was performed to understand such discrepancies.

Next, Moore et al. (2010) reported the IR spectra of numerous nitrile ices from 30 cm^{-1} to 5000 cm^{-1}. The investigators observed the ν_{13} band of crystalline C_2H_5CN ice spectrally peaking at 220.9 cm^{-1}, obtained under similar experimental conditions as that of Dello Russo and Khanna (1996), with deposition and annealing temperatures at 50 K and 140 K, respectively, and a 90 min annealing duration (see Table 1). Finally, a recent study of crystalline propionitrile ice particles generated under simulated Titan temperature and pressure conditions by collisional cooling in an optical cell cooled to 95 K, 110 K and 130 K (Ennis et al., 2017), reported the ν_{13} band centered at 226 cm^{-1} for the three temperatures studied, which is in agreement with the work of Dello Russo and Khanna (1996), and thus inconsistent with the 221 cm^{-1} spectral peak of the Haystack emission feature. Couturier-Tamburelli et al. (2018a) focused their C_2H_5CN ice study in the mid-IR region (650–5000 cm^{-1}; 15.4–2.0 μm) and therefore did not report results for the ν_{13} bending mode of the crystalline propionitrile ice that they obtained in laboratory. Table 1 summarizes the Titan-relevant laboratory works conducted for propionitrile ice over the last two decades.

The results obtained from laboratory measurements carried out up until now are generally in agreement that the ν_{13} band of propionitrile does not reproduce the spectral width and strength of the Haystack emission feature. Additionally, some of these works find that propionitrile ice is also a poor candidate for the Haystack due to the presence of the strong lattice vibrations of pure C_2H_5CN ice between 86 and 140 cm^{-1} (Dello Russo and Khanna, 1996), which are not visible in CIRS far-IR spectra (de Kok et al., 2007; Samuelson et al., 2007). de Kok et al. (2008) also report that a mixing ratio of at least 1×10^{-6} for C_2H_5CN gas is necessary if the Haystack's composition strictly contained propionitrile ice, formed via the condensation of its vapor; this mixing ratio requirement is about three orders of magnitude higher than the ALMA-observed amount of propionitrile vapor in Titan's stratosphere (Cordiner et al., 2015).

Table 1

Summary of laboratory experiments of propionitrile (C_2H_5CN) ice for the study of Titan's stratospheric ice clouds.

C_2H_5CN Ice phase	Experimental conditions	Spectral range	Published work
Crystalline	Deposition temperature: 50–100 K Annealing: 30–180 min at 140 K Post-cooling: 35 K, 95 K	80–5000 cm^{-1}	Dello Russo and Khanna (1996) Dello Russo (1994)
	Deposition temperature: 60–80 K Annealing: 4–5 h at 100–120 K Post-cooling: 15 K, 50 K, 80 K Post-warming: 150 K, 160 K	200–7800 cm^{-1}	Khanna (2005a)
	Deposition temperature: 50 K Annealing: 90 min (mid-IR) at 140 K 92 min (far-IR) at 140 K Post-cooling: 20 K, 35 K, 50 K, 75 K 95 K, 110 K	30–5000 cm^{-1}	Moore et al. (2010)
	Deposition temperature: 140 K	30–5000 cm^{-1}	Moore et al. (2010)
	Collisional cooling cell (N_2 cold bath gas) Aerosols ice particles formed at 95 K, 110 K, 130 K	50–5000 cm^{-1}	Ennis et al. (2017)
	Deposition temperature: 20 K Post-warming: 95 K, 110 K, 125 K	650–5000 cm^{-1}	Couturier-Tamburelli et al. (2018a)
	Deposition temperature: 30 K Post-warming: 150 K	50–600 cm^{-1}	Ennis et al. (2018)
Amorphous	Deposition temperature: 50 K Post-warming: 75 K, 95 K, 110 K	30–5000 cm^{-1}	Moore et al. (2010)
	Deposition temperature: 20 K	650–5000 cm^{-1}	Couturier-Tamburelli et al. (2018a)
	Deposition temperature: 30 K	50–600 cm^{-1}	Ennis et al. (2018)

As noted above, previous laboratory works of propionitrile ice, especially for the crystalline phase, are inconsistent in the spectral position assignment of the ν_{13} bending mode of crystalline propionitrile ice, with a frequency shift in the band position up to 5 cm^{-1}. This may be indicative of the non-reproducibility of the transmission spectroscopy results, which may arise from variable experimental conditions but more likely, this is a result of a poor understanding of its phase behavior due to incomplete studies of the ice evolution with temperature and time. For example, in the previous experimental studies on propionitrile, we observe a discrepancy in the annealing temperature and annealing time duration necessary to achieve its crystalline phase (see Table 1). While both Moore et al. (2010) and Dello Russo and Khanna (1996) annealed propionitrile ice at 140 K but with different annealing time durations (90 min and 30–180 min, respectively), the study by Khanna (2005a) annealed the ice at 120 K for 4–5 h. These experimental discrepancies raise concerns about the correct crystalline phase of C_2H_5CN ice. Spectral variabilities observed in the experimental results also affects the optical constants of the ice being studied, i.e. the real (n) and imaginary (k) parts of the complex refractive indices, which are needed for radiative transfer fits to Titan's observed spectra.

Therefore, in order to accurately determine the potential role of propionitrile in the formation and composition of Titan's stratospheric ice clouds, particularly the chemically unidentified Haystack emission feature, along with the known discrepancies from all previous propionitrile ice laboratory works, we found it necessary to carry out a comprehensive study on this cyanide. We also briefly discuss the significance of our ongoing co-deposition experiments, in which we are now investigating the spectral behavior of propionitrile ice when it becomes part of a two-compounds (binary) and/or three-compounds (ternary) co-condensed mixture. These co-condensed ice studies are necessary since (1) Titan's CIRS-observed stratospheric ice clouds appear to contain ice mixtures that result from co-condensation, as opposed to strictly layered with single, pure chemical compounds (Anderson and Samuelson, 2011; Anderson et al., 2016, 2018a, 2018b), and (2) we must examine if the low energy bands of propionitrile ice become altered by the surrounding molecules when mixing occurs. Indeed, using HCN ice as an example, we have found that its strong

librational lattice mode is suppressed when HCN is mixed with prevailing C_2N_2 in the co-condensed ice (Anderson et al., 2018a).

2. Experimental method

2.1. Sample preparation and purification

Simulating Titan's stratospheric ice cloud environment in the laboratory requires forming Titan ice analogs with high purity and free of oxygen-bearing components. The propionitrile we used in this Titan ice study was purchased as liquid, and although its purity is certified as 99.98%, it still needs to be purified from air contaminants, such as water from atmospheric humidity and carbon dioxide (CO_2), prior to the onset of experiments. The presence of any impurity in a sample will alter the spectral features of the Titan ice analog, which ultimately yields incorrect refractive indices. Purifying the sample then becomes crucial. Unfortunately, most of the published laboratory work focused on Titan's stratospheric ice analogs contains relative degrees of impurities, with little effort dedicated to sample purification. For example, in the C_2H_5CN ice experiments of Khanna (2005a), the investigator did not perform purification on the purchased liquid propionitrile and H_2O contamination was detected in the resulting absorbance spectra. Moreover, in the IR spectra of Ennis et al. (2017) collected for C_2H_5CN ice particles (generated from the purchased liquid C_2H_5CN), the presence of both CO_2 and formic acid was visible, in which the former was introduced as an impurity in the dry N_2 gas bath, while the latter was present as an adsorbed remnant from previous enclosive flow cooling (EFC) cell experiments. As well, the Ennis et al. spectra contain traces of acetonitrile, introduced via absorption on the EFC cell or the deposition line walls. In this present work, we provide laboratory IR absorbance spectra, along with their corresponding refractive indices, of highly purified amorphous and crystalline propionitrile ices.

Propionitrile (Fluka, 99.98%) used in this present study was purified by freeze-pump-thaw cycling under vacuum using a cold bath at −116 °C (157 K) made from a mixture of ethanol (C_2H_5OH) and liquid nitrogen (LN_2). As mentioned above, purification is critical in order to remove air contaminants, predominantly H_2O and CO_2, as well as other
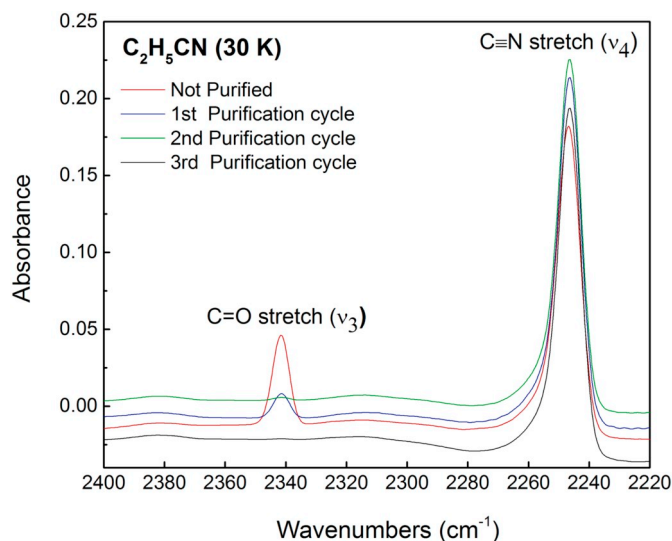
Fig. 1. Mid-IR absorbance spectra of amorphous C_2H_5CN ice (vapor deposited at 30 K), indicated by the ν_4 C≡N stretch absorption band at 2246 cm^{-1}. The four colour-coded curves depict various degrees of CO_2 contamination (shown by the ν_3 C=O stretch absorption band at 2342 cm^{-1}) in the C_2H_5CN sample, following numerous freeze-pump-thaw cycles under vacuum using a -116 °C C_2H_5OH/LN_2 cold bath. The red curve shows a 4.2 μm thick film of C_2H_5CN ice for the unpurified C_2H_5CN sample, which contains a significant amount of CO_2. The blue curve shows the ice film of the same C_2H_5CN sample (with the same thickness as previously) following five freeze-pump-thaw cycles (1st purification cycle), with a reduced amount of CO_2 visible in the spectrum. The green curve of C_2H_5CN ice film is obtained after four additional freeze-pump-thaw cycles (2nd purification cycle), with CO_2 now visible as a trace contaminant in the C_2H_5CN ice sample. The black curve shows the final purified C_2H_5CN ice spectrum, after a total of thirteen freeze-pump-thaw cycles (3rd purification cycle), with the amount of CO_2 contamination now below the FTIR spectrometer detection limit. (For interpretation of the references to colour in this figure legend, the reader is referred to the web version of this article.)

trace organic impurities. After purification, the pure C_2H_5CN sample was transferred in vacuo to a 42 ml leak-tight vacuum Schlenk glass tube equipped with a variable leak valve, then frozen at -196 °C (77 K) under a LN_2 bath, and finally stored inside a -86 °C (187 K) freezer. The purity of propionitrile was inspected in the resulting mid-IR absorbance ice spectra after vapor deposition at 30 K and 110 K by looking for any impurity absorption bands. Example C_2H_5CN absorbance spectra are shown in Figs. 1 and 2, demonstrating the need for several freeze-pump-thaw cycles under vacuum with a C_2H_5OH/LN_2 cold bath to totally remove the CO_2 and H_2O contaminants (and other trace impurities) from the C_2H_5CN sample.

2.2. Acquisition of the infrared spectra of propionitrile thin ice films

All propionitrile experiments were conducted using the SPECtroscopy of Titan-Related ice AnaLogs (SPECTRAL) ice chamber (Fig. 3), located in the Spectroscopy for Planetary ICes Environments (SPICE) laboratory at NASA Goddard Space Flight Center (GSFC). The detailed description of the SPECTRAL ice chamber, along with the standard experimental methodology for vapor deposition and data analysis utilized here, are given in Anderson et al. (2018a).

In this present work, we have performed thin film transmission spectroscopy of the amorphous to crystalline phases of pure propionitrile ice, from the far- to near-IR spectral region (50–11,700 cm^{-1}; 200–0.85 μm), as functions of temperature and time. As well, we have determined their corresponding optical constants. The spectra were collected under a vacuum of 8×10^{-8} mbar at low deposition temperatures, ranging from 30 K to 160 K. For each spectrum, 256 scans were averaged at a spectral resolution of 4 cm^{-1}. The FTIR
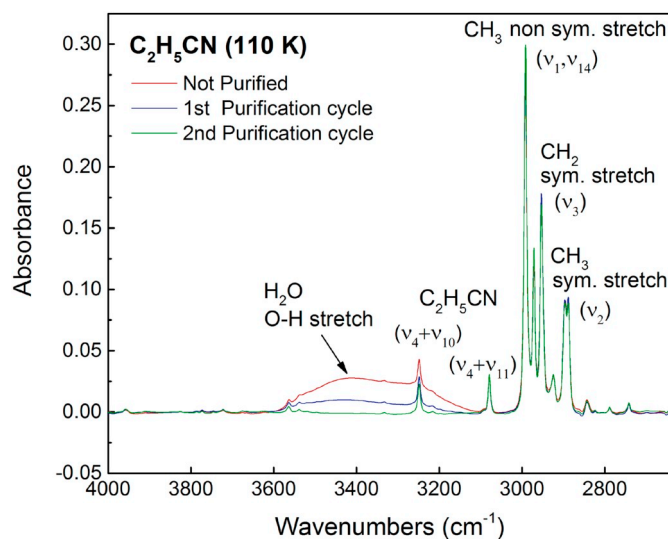

Fig. 2. Mid-IR absorbance spectra of C_2H_5CN ice (vapor deposited at 110 K), indicated by the ν_2 CH$_3$ and CH$_2$ symmetric stretch absorption bands at 2288–2896 cm^{-1} and 2953–2971 cm^{-1}, respectively; as well as by the ν_1, ν_4 CH$_3$ asymmetric stretch absorption band at 2992 cm^{-1} and the $\nu_4 + \nu_{11}$, $\nu_4 + \nu_{10}$ vibration modes at 3079 cm^{-1} and 3249 cm^{-1}, respectively. The three colour-coded curves depict various degrees of H_2O contamination (shown by the broad O–H stretch absorption band between 3200 and 3600 cm^{-1}) in the C_2H_5CN sample, following numerous freeze-pump-thaw cycles under vacuum using a -116 °C C_2H_5OH/LN_2 cold bath. The red curve shows a 3.6 μm thick film of C_2H_5CN ice for the unpurified C_2H_5CN sample, which contains a significant amount of H_2O. The blue curve shows the ice film of the same C_2H_5CN sample (with the same thickness as previously) following nine freeze-pump-thaw cycles (1st purification cycle), with a reduced amount of H_2O visible in the spectrum. The green curve of C_2H_5CN ice film shows the final purified C_2H_5CN ice spectrum obtained after four additional freeze-pump-thaw cycles (2nd purification cycle), giving a total of thirteen freeze-pump-thaw cycles, with the amount of H_2O contamination now below the FTIR spectrometer detection limit. (For interpretation of the references to colour in this figure legend, the reader is referred to the web version of this article.)

spectrometer has three different beamsplitter/detector combinations depending on the spectral range in which the spectra are acquired. For the far-IR spectral region (50–700 cm^{-1}; 200–14.3 μm), a DTGS detector with a polyethylene window is combined with a solid substrate beamsplitter. For the mid-IR spectral region (600–8000 cm^{-1}; 16.7–1.25 μm) a MCT-A detector with a KBr beamsplitter is used. For the near-IR spectral region (1000–11,700 cm^{-1}; 10–0.85 μm), the MCT-A detector is coupled to a CaF$_2$ beamsplitter using the white light source (an IR source is used for the far- and mid-IR spectral regions). When collecting the mid-IR spectra of propionitrile ice, the FTIR spectrometer's gain and aperture size were first optimized in the mid-IR to reduce the intensity of the CVD diamond absorption bands arising from the sample substrate and chamber windows. This correction is necessary since CVD diamond strongly absorbs between 2300 cm^{-1} and 2000 cm^{-1}.

Prior to vapor deposition, background spectra were collected for each selected temperature. Ice absorbance spectra were then recorded after they were automatically background corrected, which takes the ratio between the individual ice and background spectra, thus removing spectral features introduced by the spectrometer and also the atmospheric gases. This procedure provides a final ice absorbance spectrum with peaks arising solely from the ice sample. The baseline of this final IR ice absorbance spectrum contains channel fringes, which are produced by the reflections at the vacuum-ice and ice-substrate sample surface (Hirschfeld and Mantz, 1976). The channel fringes behave somewhat like a sinusoidal waveform, with the ice spectral features superimposed. Prior to the calculation of the real and imaginary parts of
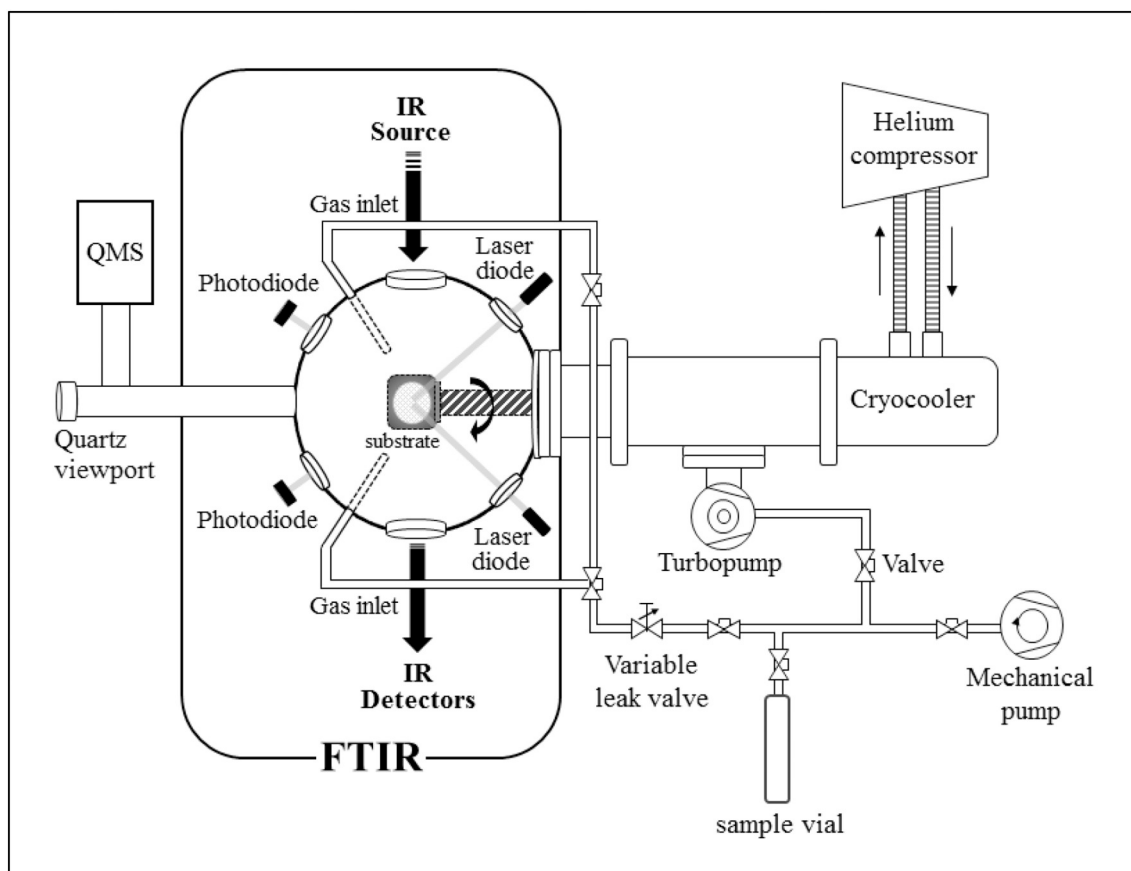
Fig. 3. Schematic illustration of the experimental setup used for the C_2H_5CN ice experiments in the SPECTRAL ice chamber (modified from Anderson et al., 2018a). Vapor deposition of C_2H_5CN onto a cold diamond substrate (30 K – 160 K) forms a thin ice film that is monitored in situ by IR transmission spectroscopy from $50\,cm^{-1}$ to $11,700\,cm^{-1}$ (200–0.85 μm) through a FTIR spectrometer. Double laser interferometry is used to determine the thickness of the ice films.

the ice refractive index, *n* and *k*, each laboratory measured IR absorbance spectrum is corrected to remove the channel fringes. When removing the channel fringes from all spectra acquired, we purposely set up the absorbance value to zero in the Far-IR region for frequencies below $55\,cm^{-1}$ when the signal-to-noise (S/N) becomes low (S/N < 3) and the peaks cannot be accounted as real absorption bands. Once the spectra are channel fringe corrected, the optical constants *n* and *k* are then computed using a custom-developed IDL program which uses the Beer-Lambert law and applies an iterative Kramers-Kronig analysis of the laboratory corrected absorbance spectra (see Anderson et al., 2018a for the data processing details). The absorbance spectra and optical constants are available on the SPICE laboratory website at https://science.gsfc.nasa.gov/691/spicelab.

At room temperature (295 K), propionitrile has a saturation vapor pressure of 53 mbar. As a result, vapors of pure propionitrile were then easily obtained at saturation equilibrium from the purified liquid phase (stored in the closed sample Schlenk tube) evaporated at room temperature. Pure C_2H_5CN gas was then flowed through two stainless steel gas deposition lines into the spherical sample compartment of the SPECTRAL chamber at a flow rate of 4.2 ml/min, and then slowly condensed onto a diamond substrate at the desired low temperature, with an ice deposition rate of 0.35 μm/min. Warming and cooling rates of the diamond substrate on which the ice deposits were about $3\,K\,min^{-1}$. The cooling/heating of the diamond substrate inside the sample chamber is performed by a close cycle cryostat which contains a cryocooler connected to an air-cooled helium compressor. The temperature is controlled by a temperature controller connected to the cryocooler, a 36 Ohm internal resistive Thermofoil heater and two silicon diodes (uncalibrated temperature sensors; accuracy ± 0.5 K from 2 K to 305 K) located on the holder of the diamond substrate (see more

details in Anderson et al., 2018a). The thicknesses of the ice films were determined by double laser interferometric technique (detailed in Anderson et al., 2018a) and ranged between 3.7 and 4.2 μm. Thick ice films of 7 μm and 10 μm were also grown in experiments when the deposition temperature was set at 140 K, 150 K and 160 K in order to study the C_2H_5CN ices as they started to sublime (≥ 140 K).

We also initiated a few experiments of co-condensed ices containing mixtures of HCN, C_6H_6, and C_2H_5CN, which initiated a new investigation aimed at identifying the chemical composition of the Titan's CIRS-observed Haystack emission feature. Specifically, we have begun a detailed investigation to determine if co-condensed ices can account for the chemical composition of the Haystack. The gas mixtures of HCN, C_6H_6, and C_2H_5CN previously purified were prepared through a vacuum glass manifold previously pumped to 6×10^{-6} mbar. HCN was synthesized in our laboratory as described in Anderson et al. (2018a), while benzene (99.99%) was purchased from Sigma-Aldrich. Both were purified through several cycles of freeze-pump-thaw under vacuum using cold baths of C_2H_5OH/LN_2 ($-116\,°C$) and acetone/LN_2 ($-94\,°C$). The co-condensed ices were then obtained by depositing the gas mixtures at 110 K. The full co-condensed ice study, however, as it pertains to the Haystack's chemical composition is beyond the scope of this paper.

3. Results and discussion

3.1. Study of the crystallization of propionitrile ice

One of the initial objectives of this work was to accurately identify the temperature at which propionitrile ice transitions from its amorphous to crystalline phase. For most of the previous Titan ice studies,

the crystallization of an ice is commonly achieved by annealing the sample (Couturier-Tamburelli et al., 2018a, b; Couturier-Tamburelli et al., 2015; Moore et al., 2010; Khanna, 2005a, 2005b; Dello Russo and Khanna, 1996; Khanna, 1995; Masterson and Khanna, 1990; Khanna et al., 1990; Khanna et al., 1988; Ospina et al., 1988). This process involves depositing the vapor onto the cold substrate in the amorphous phase at very low temperatures (e.g. < 100 K), then warming the ice to its appropriate crystalline temperature, and annealing it for several hours at this temperature to allow the molecules to adopt a low-energy configuration. In previous Titan-related experimental studies on propionitrile ice, the crystalline phase was always achieved by annealing the ice sample (see Table 1). Dello Russo (1994) and Dello Russo and Khanna (1996) deposited C_2H_5CN vapor between 50 and 100 K (the exact deposition temperatures are not specified), and annealed the ice at 140 K for 30 to 180 min (the exact times are not reported), then cooled the ice to 95 K and 35 K to record the transmittance spectra. On the other hand, Khanna (2005a) deposited C_2H_5CN vapor at 60 K, annealed at 120 K for 4 to 5 h, then cooled/warmed the ice sample to 15 K, 50 K, 80 K, 150 K, and 160 K to record the absorbance spectra. Moore et al. (2010) deposited C_2H_5CN vapor at 50 K, annealed the ice sample at 140 K for 92 min in the far-IR and 90 min in the mid-IR, then cooled the ice sample to 20 K, 35 K, 50 K, 75 K, 95 K, and 110 K to record the absorbance spectra. As noted earlier, these three experimental studies on the crystalline phase of propionitrile ice differ in the annealing temperature and the annealing time duration to obtain crystalline C_2H_5CN (see Table 1). This raises uncertainties as to the crystallinity of their propionitrile ice samples. We therefore began our initial study on propionitrile ice by repeating these previous laboratory experiments to examine the reproducibility of the crystalline phase propionitrile results (Fig. 4).

As Fig. 4 demonstrates, we were unable to reproduce the IR absorbance spectra obtained by both Dello Russo (1994) and Khanna (2005a) when we used the same deposition and annealing temperatures, as well as the annealing time duration. Specifically, the ν_{13} and ν_{20} C-C ≡ N planar and out-of-plane bending modes reported by Dello Russo (1994) are shifted by several wavenumbers compared to our spectrum; the lattice vibration band is shifted as well and appears significantly broader. The Khanna (2005a) spectrum also shows a frequency shift in the ν_{12} C-C-C skeletal bending mode, while in Dello Russo and Khanna (1996), this absorption band splits into two peaks (not shown in Fig. 4 but is reported in their Table III). Moreover, compared to Khanna (2005a), our absorbance spectrum shows an additional IR band at 277 cm^{-1}, which we identified as the ν_{21} CH$_3$ torsional fundamental. We are the first to report this torsional mode in C_2H_5CN ice since this band has only been previously reported in the IR spectrum of liquid propionitrile (Duncan and Janz, 1955). We were able, however, to adequately reproduce the IR absorbance spectra obtained by Moore et al. (2010), with only two main noticeable differences: (1) there is a small shift of 1 cm^{-1} in the ν_{12} C-C-C bending mode, and (2) we observe a split of the C_2H_5CN lattice band into two or three peaks that was not reported by Moore et al. Dello Russo and Khanna (1996) did report a split of the C_2H_5CN lattice band into six peaks (listed in their Table III), whereas Dello Russo (1994) only observed a single split. Lastly, Khanna (2005a) did not detect the lattice mode of C_2H_5CN ice since the absorbance spectra were only collected from 200 cm^{-1} to 4000 cm^{-1}.

The discrepancies between our laboratory spectra of annealed crystalline C_2H_5CN ice and the previous works demonstrate a non-reproducibility of the experimental results when the annealing technique is used to achieve the crystalline ice phase of propionitrile.

We also point out that in the experiments of Dello Russo (1994), Dello Russo and Khanna (1996), Khanna (2005a), and Moore et al. (2010), a polyethylene substrate was used to deposit the propionitrile vapors at low temperature, whereas the SPECTRAL chamber incorporates a diamond substrate for vapor deposition. Diamonds are extremely efficient thermal conductors as compared to polyethylene

material, and it cannot be ruled out that the temperature measured at the substrate location in the previous experiments may have yielded incorrect values by a few Kelvin.

Apart from the collisional cooling cell experiments performed by Ennis et al. (2017), all of the other previous laboratory studies related to the study of propionitrile ice have analyzed its crystalline phase by first depositing the vapor at cold temperatures (≤ 60 K), then annealing the samples at temperatures ≥ 120 K, and finally cooling the ice to lower temperatures to record the absorbance spectra. This experimental approach, although commonly used to study ices formed in the interstellar medium, is not appropriate for simulating ices formed in Titan's stratosphere. In order to reproduce ice cloud formation in Titan's stratosphere, vapors must be directly deposited at warmer temperatures (e.g., 110 K), since most of Titan's organic vapors condense as the vapors cool while descending throughout Titan's stratosphere. In the Moore et al. (2010) study, the investigators briefly reported that the spectra of crystalline C_2H_5CN obtained by direct vapor deposition at 140 K appeared different from that of C_2H_5CN ice annealed at 140 K for 90 min. They observed changes in the band positions, shape and intensities, and particularly indicated that the ν_8 CH$_2$ wag band had split, and also noted large shifts to higher energies in the ν_5, ν_{16}, and ν_6 CH$_3$ and CH$_2$ deformation bands, with small changes in the ν_4 C≡N stretching mode. However, Moore et al. (2010) did not carry out any further investigation on these observations, and only reported the optical constants n and k for the annealed crystalline phase of C_2H_5CN ice. Couturier-Tamburelli et al. (2018a) reported a short analysis, in the mid-IR region, on the influence of temperature on propionitrile ice when warming amorphous C_2H_5CN ice (see Table 1). C_2H_5CN vapor was deposited at 20 K and then warmed up to 300 K, at a heating rate from 0.8 to 2 K min^{-1}. They indicated that, when heated, C_2H_5CN ice undergoes three crystallization transition phases with observed spectral changes (i.e. band shifts and band splits); one starting at 95 K, the second at 110 K and the last one at 125 K. They provided the temperature-dependence spectra at 95 K, 110 K and 125 K in three narrow mid-IR spectral regions: 1250–1500 (8.0–6.7 μm), 2220–2280 (4.5–4.4 μm), and 2800–3100 (3.6–3.2 μm). Couturier-Tamburelli et al. (2018a) did not report any investigation on the time-dependence spectral variations of their warmed C_2H_5CN ices.

In this present work, we have performed a comprehensive infrared study of propionitrile ice, from the amorphous to the crystalline phase, by direct deposition of the vapors at temperatures ranging from 30 K to 160 K. For each deposition temperature, we have examined the temporal variation of the C_2H_5CN absorption bands from the far- to near-IR spectral region, in an effort to better understand the C_2H_5CN ice phase transitions with the corresponding observed spectral changes and to identify when the complete crystallization of propionitrile ice is achieved. Specifically, we have recorded absorbance spectra at deposition temperatures of 30 K, 60 K, 90 K, 110 K, 120 K, 125 K, 130 K, 135 K, 140 K, 150 K, and 160 K, as well as studied the ice evolution with time after deposition (Figs. 5, 6, 8 and 9). Although the absorbance spectra presented here focus on the far-IR spectral region (to study Titan's CIRS-observed far-IR ice clouds), we have also collected the absorbance spectra at these temperatures and times after deposition in the mid- and near-IR (600–11,700 cm^{-1}/16.7–0.85 μm). They are available on the SPICE Lab website mentioned above. However, in the spectral region 8000–11,700 cm^{-1} (1.25–0.85 μm), for ice film thicknesses ranging from 3.7 to 4.2 μm, propionitrile ice did not show any absorption bands.

The amorphous phase of C_2H_5CN ice was identified from 30 K to 90 K (Fig. 5). The spectra at this temperature range show that after several hours following vapor deposition, there are no observed changes in the band positions, band intensities, or in the band shapes, in any of the absorption bands due to intramolecular vibrations. In the lower energy part of the far-IR (< 150 cm^{-1}), the lattice absorption band is slightly affected by the deposition temperature, with a band shift of 5 cm^{-1} to higher frequencies as temperature increased from
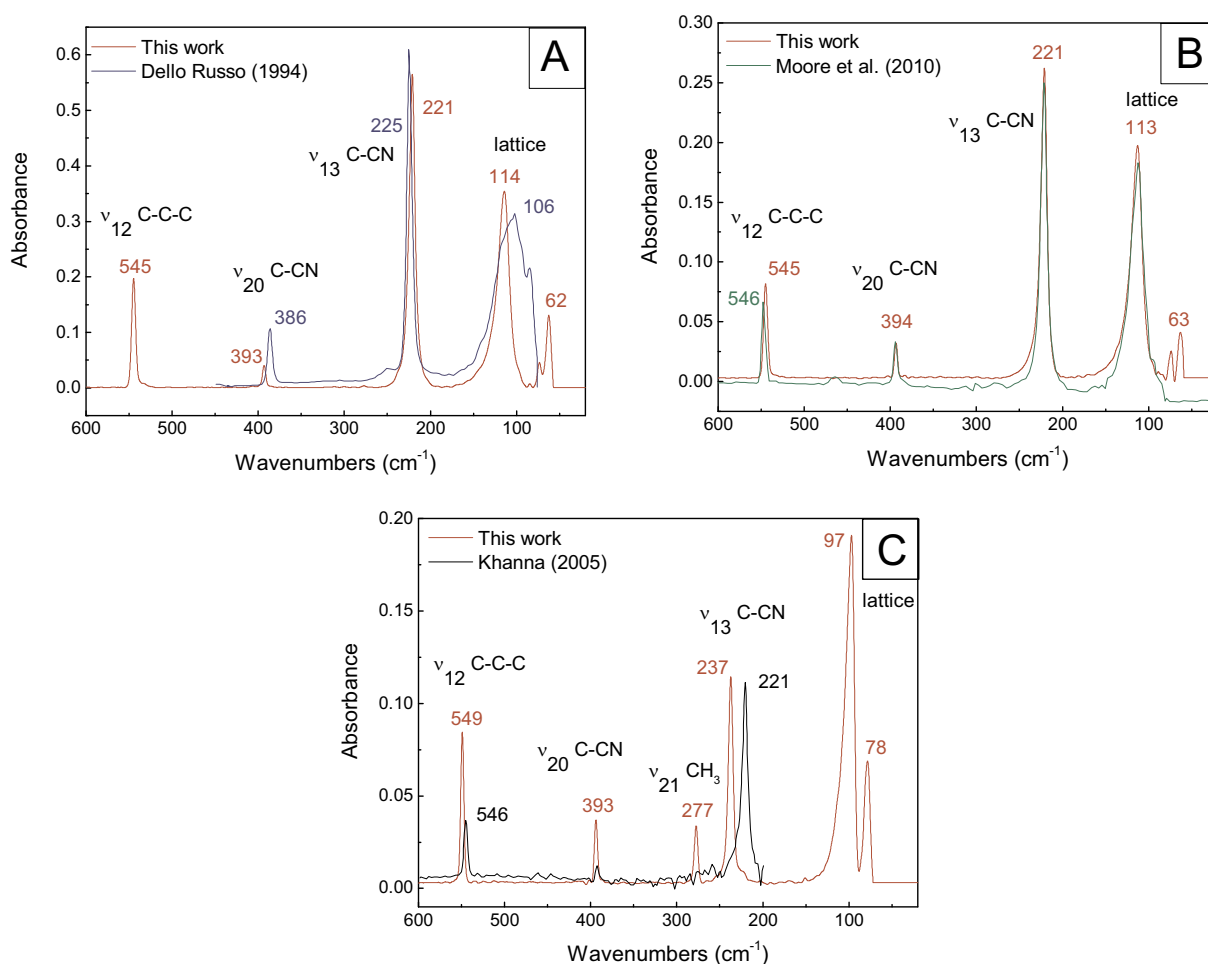
Fig. 4. Comparisons of absorbance spectra of annealed crystalline C_2H_5CN ice between previous experimental studies to those obtained under similar experimental conditions using the SPECTRAL chamber in the SPICE laboratory (current work). (A) The blue curve shows the Dello Russo (1994) absorbance spectrum at 95 K, while the red curve depicts the absorbance spectrum at 95 K from this work, in which C_2H_5CN vapor was deposited at 60 K, annealed at 140 K for 180 min, then cooled to 95 K. (B) The green curve depicts the Moore et al. (2010) absorbance spectrum at 95 K, while the red curve shows the absorbance spectrum at 95 K from this work, in which C_2H_5CN vapor was deposited at 50 K, annealed at 140 K for 90 min, then cooled to 95 K. (C) The black curve shows the Khanna (2005a) absorbance spectrum at 80 K, while the red curve shows the absorbance spectrum at 80 K from this work, in which C_2H_5CN vapor was deposited at 60 K, annealed at 120 K for 240 min, then cooled to 80 K. Superimposed in each figure are the vibrational transitions and peak frequencies for each observed ice absorption band. (For interpretation of the references to colour in this figure legend, the reader is referred to the web version of this article.)

30 K to 90 K. This spectral behavior is expected. It is known that in a crystalline solid, the higher the temperature of the solid, the more intensively its atoms or groups of atoms oscillate about an equilibrium position in the crystal structure, which directly affects the spectral properties of the lattice vibrations. Spectral changes due to temperature occur not only in crystalline ice structures but also in disordered (amorphous) solids, since amorphous networks exhibit internal degrees of freedom (Hunklinger, 1982). In an amorphous solid, the periodic lattice structure does not exist but intramolecular interactions and interactions among molecules in the ice are strong. In this case, the change of the temperature of the amorphous ice produces as well spectral shifts of the lattice mode. At 90 K and at 18 h post-deposition, the lattice mode shifts even more, by almost $10\,cm^{-1}$ compared to 30 K, and the broad amorphous lattice feature starts to sharpen. As well, a new vibrational band, the ν_{21} methyl (CH_3) torsional fundamental peaking at $263\,cm^{-1}$, not observed at 30 K nor at 60 K, starts to appear at 90 K at 18 h post-deposition. Although, as stated earlier, we are the first to report this torsional mode in the C_2H_5CN solid phase, Heise et al. (1981) reported that the CH_3 torsion of propionitrile in the gas phase can be obscured by the much stronger ν_{13} $C\text{-}C\equiv N$ skeletal bending band of gaseous C_2H_5CN peaking at $207\,cm^{-1}$. Previous works carried out for propionitrile ice, have indicated the ν_{21} CH_3 torsional mode

combining at the same frequency as the ν_{13} bending mode (Dello Russo and Khanna, 1996; Ennis et al., 2017). Those studies were not as comprehensive and methodical as our present work, where we analyze for the first time, the evolution of C_2H_5CN ice spectra with time (from just after deposited and every hour, up to 24 h after deposition) at various temperatures, from 30 K to 160 K. Such detailed study is critical to observe the ν_{21} torsional band. As well, our spectroscopic setup in the far-IR region, which combines a DTGS/polyethylene detector with a solid substrate beamsplitter detector and uses a diamond substrate and diamond transmission windows, has a much better resolution than the previous published experimental setups, enhancing the sensitivity of our FTIR spectroscopy to detect weaker absorption bands in the Far-IR.

Fig. 6 depicts the absorbance spectra of propionitrile ice deposited at 110 K, 120 K and 125 K and shows the observed spectral variations in the absorption band position and band shape with deposition time.

At 110 K and 120 K, the ν_{21} CH_3 torsional band at $261\,cm^{-1}$ and $260\,cm^{-1}$, respectively, is present in the spectra just after the vapor has been deposited and shifts to higher energies by $15\,cm^{-1}$ 24 h after deposition. This torsional mode at 125 K does not undergo any band shift; its peak remains at $275\,cm^{-1}$ just after vapor deposition and resides at this exact frequency for 24 h post-deposition. For all three deposition temperatures, the ν_{13} $C\text{-}C\equiv N$ in-plane bending band of
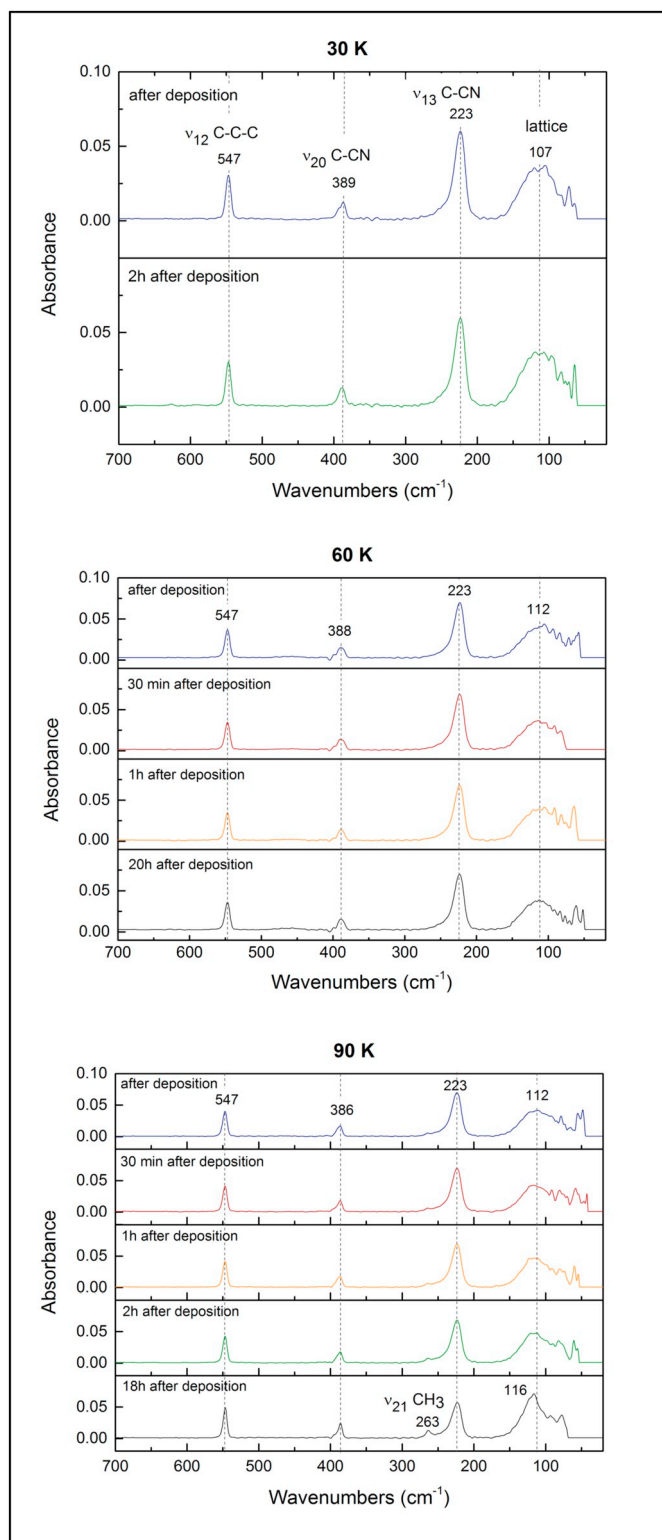
Fig. 5. Temperature and time evolution (up to 20 h after deposition) of far-IR absorbance spectra of amorphous C_2H_5CN ice (4 μm thick film) obtained after deposition of the propionitrile vapors at temperatures of 30 K, 60 K and 90 K. Superimposed in the figures are the vibrational transitions and/or peak frequencies for the observed ice absorption bands.

C_2H_5CN ice peaking at 225 cm^{-1} just after deposition shifts to higher energies by about 12 cm^{-1}. The C-C ≡ N out-of-plane bending mode (ν_{20}) at ~387 cm^{-1} just after deposition also undergoes a band shift to higher frequencies at 110 K, 120 K and 125 K with time, but is less

significant (by about 6 cm^{-1} at 24 h after deposition), and the ν_{12} C-C-C skeletal bending band is even less shifted (by 2 cm^{-1}) at 24 h post-deposition. The lattice vibration peaks at different frequencies just after deposition for the three temperatures: at 114 cm^{-1} at 110 K, at 110 cm^{-1} at 120 K, and at 98 cm^{-1} at 125 K, and also shifts to lower energies at 110 K and 120 K by 15 and 12 cm^{-1}, respectively, 24 h after deposition. As a function of post-deposition time, the lattice band sharpens and splits into two for all three temperatures, but occurs faster with increasing temperature. While the band shift and band split take place 24 h after deposition at 110 K, they start after 46 min at 120 K, and after 15 min at 125 K.

It has been reported in many ice crystallization experiments that generally, upon crystallization, a sharpening of some of the infrared absorption bands are observed (Moore and Hudson, 1994, 1992; Hardin and Harvey, 1973; Bertie and Whalley, 1967). The band sharpening we observe for the lattice mode of propionitrile ice with time after deposition indicates that the molecules start to reorder. As well, the significant band shifts observed in the methyl torsion (ν_{21}) indicates that the CH$_3$ group is reordering and/or reorienting in the C_2H_5CN molecules. The reordering of the molecules of propionitrile are transitioning into a lower energy state.

As pointed out by Duncan and Janz (1955) and Khanna (2005a), hydrocarbons and organic molecules that contain methylene (CH$_2$) and methyl groups have low barriers to rotation in adjacent singly bonded carbon atoms. As a consequence, such molecular samples cooled down at low temperatures produce several possible orientations of these groups in the solid phase, which may mostly still be amorphous. The sample may then undergo some intermediate phase transitions as well, which we observe in the spectra collected at 110 K, 120 K and 125 K, with the appearance of the ν_{21} torsional band observed only at these three temperatures.

To reach the crystalline phase, the dipole moment of the molecule also dictates the orientation of the molecules and their packing. Non-symmetric molecules containing nitrogen possess significant dipole moments, which in turn dictates physical parameters such as condensation temperatures, intermolecular interactions during the nucleation, etc. Propionitrile, as part of this group of molecules, has a large permanent dipole moment with a value of 4.00 μ (Hurdis and Smyth, 1943) due to induction attributed to the polar nature of the C≡N group. Actually, the large permanent dipole of the C_2H_5CN molecule results in strong absorptions due to lattice vibrations, and may also be responsible for the possible reorientations of the molecule.

At temperatures between 110 K and 130 K, we observe that the spacing between the channel fringe maxima in the IR spectra increases with time, indicating that the thickness of the ice film decreases with time (Fig. 7). This effect is not explained by the ice sample loss by sublimation since we have observed that C_2H_5CN ice starts to sublime at 140 K (as described below and in Fig. 8). Such an observation suggests that, while reordering, C_2H_5CN ice is compressing from its initial thickness following vapor deposition. This compression effect reduces with increasing temperature, and for temperatures ≥ 135 K, we do not observe compression of the ice with time and temperatures anymore. Due to this ice compression, for the spectra collected 24 h after deposition at 110 K, 120 K, 125 K and 130 K, it is very probable that the values of the refractive index n_0 and the thickness d, which we have computed using the laser interference fringes (see Anderson et al., 2018a), are in all likelihood incorrect. We are currently developing a program to compute the ice thickness from the IR spectra, with the ice thickness only dependent on the wavenumber spacing between maxima and the real part of the refractive index of the ice. These results will provide a good approximation of the new ice film thickness at 24 h after deposition. We will dedicate a focused study on the ice compression at temperatures where the C_2H_5CN molecules are reordering in the ice sample, although this is beyond the scope of this current work. Such study is interesting considering that the ice compression effect could be possible on an ice particle of suspended aerosol, however it is difficult
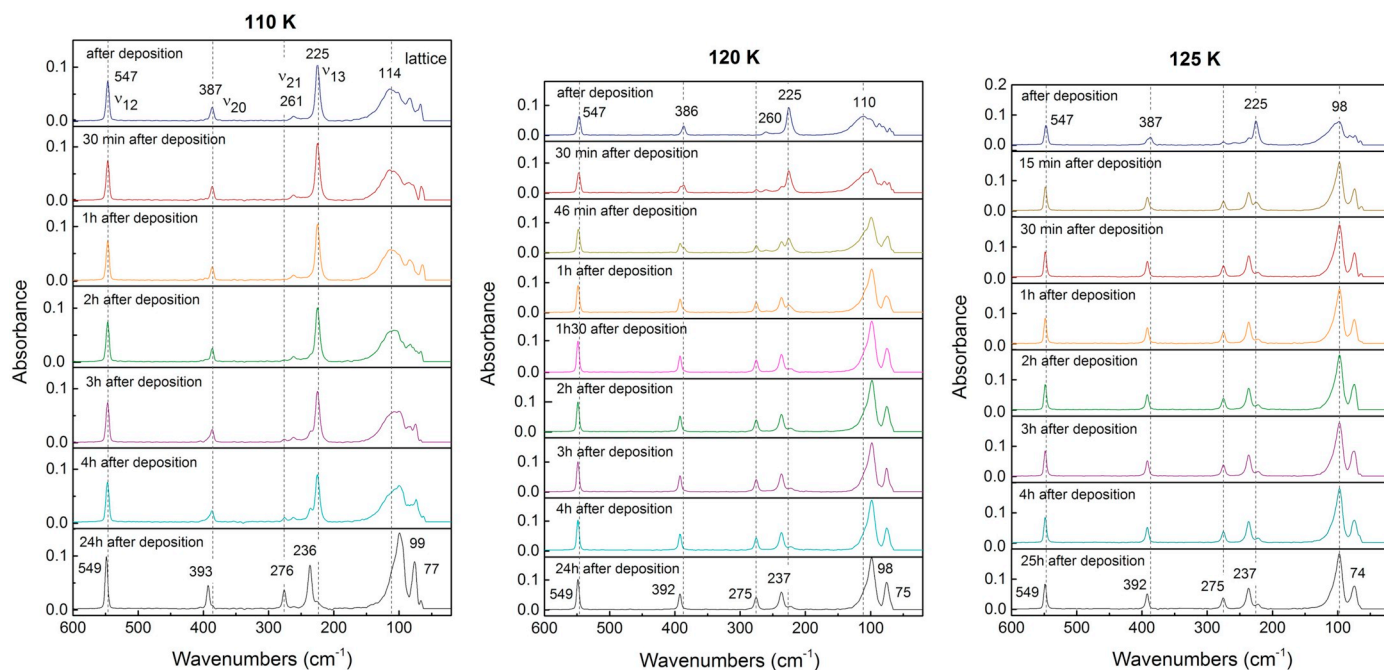
Fig. 6. Temperature and time evolution (up to 25 h after deposition) of far-IR absorbance spectra of C_2H_5CN ice (4 µm thick film) obtained after deposition of the propionitrile vapors at temperatures of 110 K, 120 K and 125 K. Superimposed in the figures are the vibrational transitions and/or peak frequencies for the observed ice absorption bands.
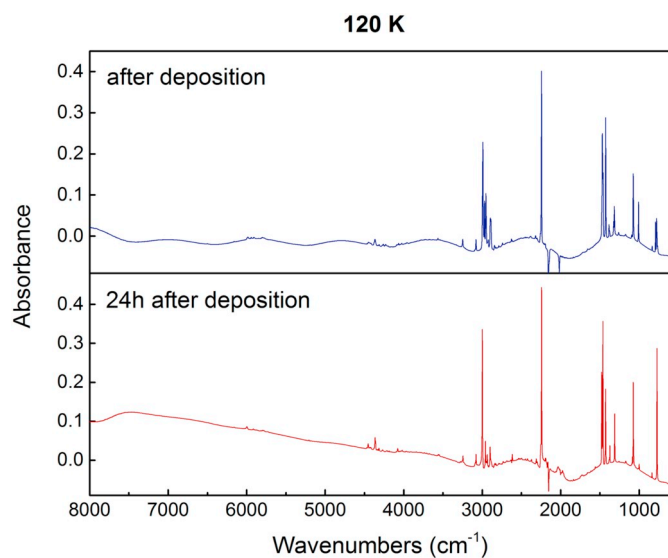

Fig. 7. Mid-IR absorbance raw spectra (channel fringe uncorrected) from $8000 \, \text{cm}^{-1}$ to $600 \, \text{cm}^{-1}$ of C_2H_5CN ice (3.84 µm thick film) obtained immediately after vapor deposition at 120 K (blue curve on top) and 24 h post-deposition (red curve at the bottom). (For interpretation of the references to colour in this figure legend, the reader is referred to the web version of this article.)

to envision that it could be tracked down through observations by remote sensing spectroscopy, because such ice compression of ice particles would be the most probably a snapshot event in time.

At temperatures higher than 125 K (Fig. 8), the ν_{21} torsional fundamental disappears. At 130 K, it still appears in the C_2H_5CN far-IR spectrum as a small band that emerges at 1 h post-deposition and remains until 69 h after deposition. But at temperatures greater than or equal to 135 K, this band is absent in the propionitrile ice spectra at all times after deposition. We interpret this observation as the completion of the reordering of the methyl group. At 135 K and 24 h post-

deposition, the frequency shift in all C_2H_5CN ice bands, except for the C-C ≡ N out-of-plane bending mode, is slight or even insignificant (by about 1 to $2 \, \text{cm}^{-1}$). The lattice mode does not undergo any shift at 135 K, while at 130 K, it shifts to higher frequencies by $5 \, \text{cm}^{-1}$ and at 140 K, it shifts to lower energies by $7 \, \text{cm}^{-1}$. The lattice band sharpens with time for the three temperatures, but the effect is less significant with increasing temperature. While at 130 K a split is still observed in the lattice band, it is almost absent at 135 K, compared to the lower temperatures (110 K, 120 K, 125 K); only a very small peak is seen beside the intense peak at $105 \, \text{cm}^{-1}$.

At 140 K and at 22 h post-deposition, the IR absorption bands of propionitrile ice have almost completely disappeared; this is due to the sublimation of the ice sample. At temperatures higher than 140 K (Fig. 9), C_2H_5CN ice sublimes very rapidly and thick ice films of 7.5 µm and 15 µm were then needed in order to collect the spectra. At 150 K with an ice film thickness of 15 µm, after 3 h post-deposition, the band intensities of propionitrile have drastically decreased by about 75%. At 160 K with an ice film thickness of 7.5 µm, all of the C_2H_5CN absorption bands have disappeared after 1 h post-deposition.

As a result of the numerous time and temperature variations observed in the absorbance spectra of propionitrile ice, it can be difficult to identify the phase transition. Previous laboratory studies on pure nitrile ices (e.g. HCN, C_2N_2, HC_3N, dicyanoacetylene C_4N_2) report a clear transition in the ice phase from amorphous to crystalline, evidenced by a change in the band shapes (splitting), an increase in band intensity, and a shift in band position (Dello Russo and Khanna, 1996; Moore et al., 2010; Khanna, 2005a). In this present propionitrile study, the crystalline temperature was assessed based on two criteria: 1) there are no observed changes (or almost no changes) in the strength and/or spectral dependence of the IR absorption bands after a 24-hour period, and 2) there is no noticeable sublimation of the ice film at the temperature held during the 24-hour time period after deposition. Based on these criteria, we have identified that propionitrile ice has completed crystallization at the deposition temperature (T_d) determined as $135 \, \text{K} \leq T_d < 140 \, \text{K}$. For this restricted temperature range, the crystalline phase of propionitrile ice is unambiguously identified from the amorphous and intermediate phases. At this temperature
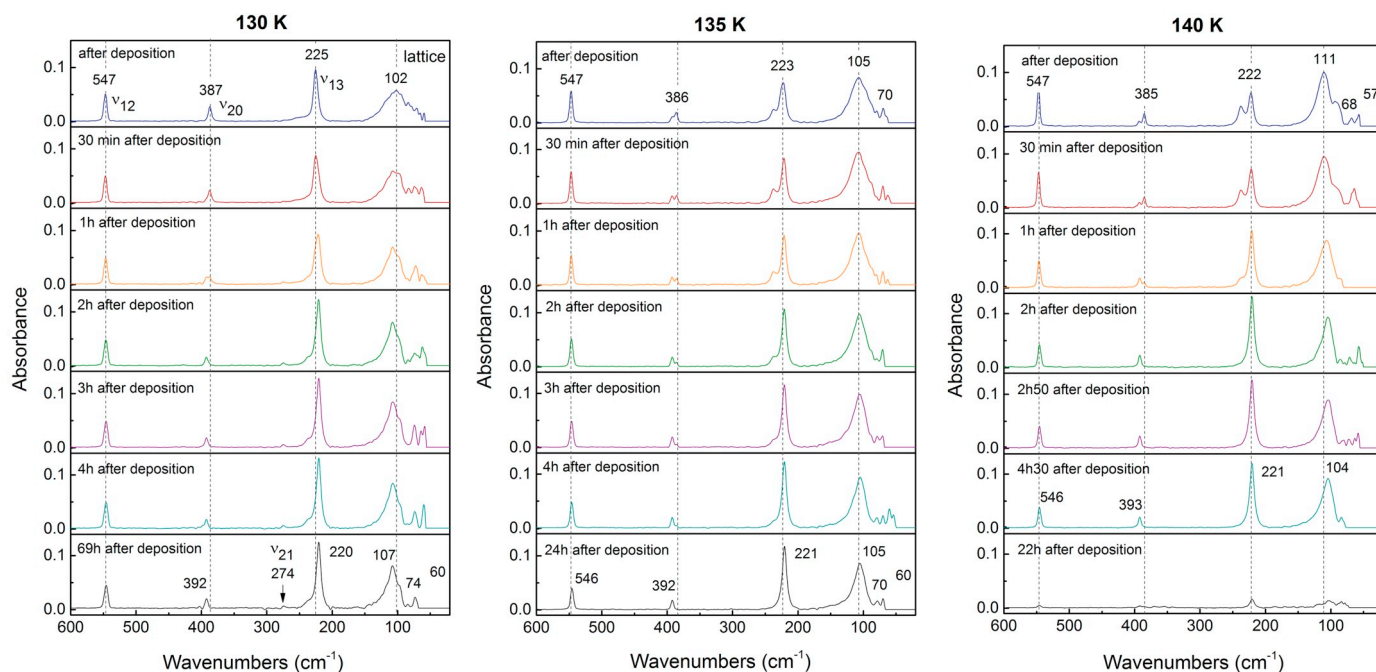
Fig. 8. Temperature and time evolution (up to 69 h after deposition) of far-IR absorbance spectra of crystalline C_2H_5CN ice (4 μm thick film) obtained after deposition of the propionitrile vapors at temperatures of 130 K, 135 K and 140 K. Superimposed in the figures are the vibrational transitions and/or peak frequencies for the observed ice absorption bands.

(135 K ≤ T_d < 140 K), the ν_{13} C–C ≡ N bending mode of crystalline propionitrile ice peaks at 221 cm^{-1}. Table 2 reports the band position of ν_{13} C–C ≡ N bending mode determined for crystalline C_2H_5CN ice in previous experimental studies and the corresponding temperature at which the crystalline phase of propionitrile has been identified.

For crystalline propionitrile ice, which was annealed at 140 K, Dello Russo and Khanna (1996) found that the ν_{12} C-C-C skeletal bending vibration split upon crystallization. We have not observed such a band splitting. Moore et al. (2010) identified as well the crystalline phase of propionitrile ice by annealing the ice at 140 K. Per our criteria to

determine the C_2H_5CN crystalline phase, we have ruled out 140 K as the correct temperature to define the crystalline phase of C_2H_5CN ice since there is significant ice sublimation at such temperature. Khanna (2005a) reported a reasonably complete crystalline C_2H_5CN ice when the sample was deposited around 60–80 K and annealed at 120 K for about 4–5 h, resulting in a spectrum that did not change subsequently until reaching 150 K (when the sample started to sublime). We have definitively ruled out 120 K as the propionitrile crystalline temperature since, as described earlier, C_2H_5CN ice undergoes significant spectral changes at this temperature with time, along with the emergence of the
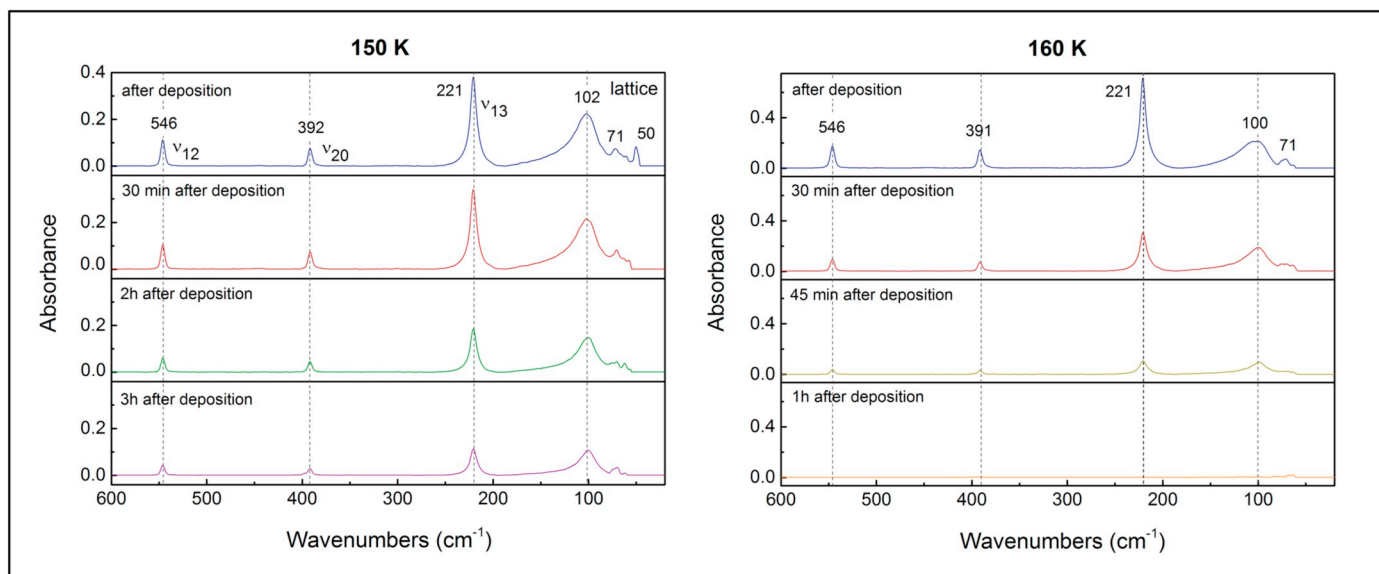

Fig. 9. Temperature and time evolution (up to 3 h after deposition) of far-IR absorbance spectra of crystalline C_2H_5CN ice obtained just after deposition of the propionitrile vapors at temperatures of 150 K and 160 K. For these temperatures, C_2H_5CN sublimes rapidly so thicker ice films of 15 μm (at 150 K) and 7.5 μm (at 160 K) were grown on the diamond substrate. Tentatively, a thick ice film ≥ 15 μm was grown and analyzed at 160 K in order to leave the sample longer than 1 h after deposition before the ice sublimed. However, several absorption bands of propionitrile appeared very saturated with such a thick sample. Superimposed in the figures are the vibrational transitions and/or peak frequencies for the observed ice absorption bands.

Table 2

Peak position of ν_{13} C–C ≡ N bending mode experimentally identified for the crystalline phase of propionitrile ice.

ν_{13} bending mode (cm^{-1})	Crystalline Temperature (K)	Published work
225	140 K (annealed, then cooled to 95 K)	Dello Russo and Khanna (1996) Dello Russo (1994)
226	140 K (annealed, then cooled to 35 K)	
221	120 K (annealed, then cooled to 15 K, 50 K, 80 K and warmed to 150 K, 160 K)	Khanna (2005a)
220.9	140 K (annealed, then cooled to 95 K)	Moore et al. (2010)
226	Aerosols ice particles formed at 95 K, 110 K, 130 K	Ennis et al. (2017)
227	150 K (annealed)	Ennis et al. (2018)
221	135 K ≤ T_d < 140 K[a]	This work

[a] In our work, the crystallization of propionitrile ice was fully completed at the deposition temperature (T_d) comprised between 135 K and 140 K (excluding 140 K, when C_2H_5CN ice sample starts to sublime).

ν_{21} CH$_3$ torsional fundamental at the side of the ν_{13} C-C ≡ N bending vibration. Rather, we have found that at 120 K, propionitrile ice is in an intermediate (or transition) phase, neither amorphous nor crystalline, where the ordering and crystal orientations of the molecules are incomplete.

Based on our criteria for the crystalline temperature of propionitrile, we have compared the spectra obtained for the annealed crystalline C_2H_5CN ice at 135 K and for the crystalline C_2H_5CN ice obtained from direct vapor deposition at 135 K (Fig. 10). The annealed sample was obtained after depositing C_2H_5CN vapor at 30 K and then annealing the ice at 135 K for 24 h.

The far-IR spectrum of crystalline C_2H_5CN ice obtained directly from vapor deposition at 135 K shows the same ν_{13} (221 cm^{-1}), ν_{20} (392 cm^{-1}) and ν_{12} (545 cm^{-1}) band frequencies as that of the C_2H_5CN ice annealed for 24 h at 135 K (after vapor deposition at 30 K); the exception is the lattice vibration that is shifted by 3 cm^{-1} to lower energies when the sample was directly deposited. We observe as well the presence of a small "tail" on the left side of the ν_{13} bending mode at 221 cm^{-1}. Given these differences between the directly-deposited crystalline ice and the annealed ice, we conclude that propionitrile ice does not reach complete crystallization when annealed at 135 K; a

complete ordering of C_2H_5CN ice is not achieved and a portion of the amorphous structure is irreversibly retained in the final crystalline phase. Khanna (2005a) pointed out the difficulty of annealing amorphous ice films of propionitrile, by requiring longer time for annealing compared to other nitriles, due to the several possible orientations of the methyl (CH$_3$) and methylene groups (CH$_2$) in the solid phase when the samples are quenched at low temperatures. We find that this trend
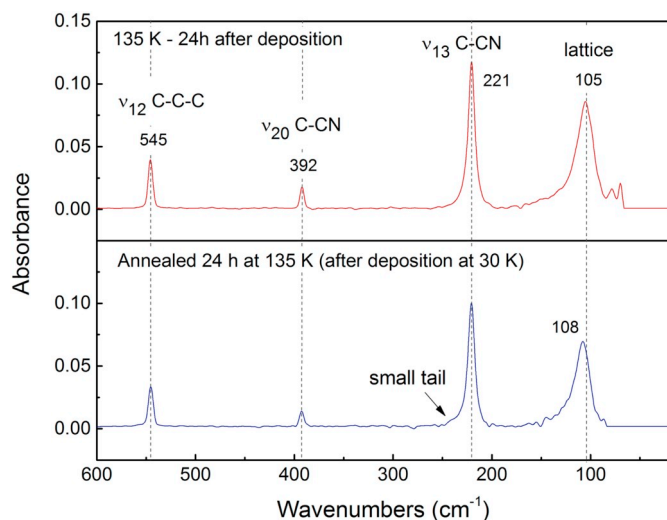

Fig. 10. Far-IR absorbance spectra of crystalline C_2H_5CN ice deposited at 135 K and held at 135 K for 24 h post-deposition (red curve on top) compared to C_2H_5CN ice deposited at 30 K and then annealed at 135 K for 24 h (blue curve at the bottom). For both samples, the ice film thickness was ~4 μm. Superimposed in the figure are the vibrational transitions and peak frequencies for the observed ice absorption bands. (For interpretation of the references to colour in this figure legend, the reader is referred to the web version of this article.)
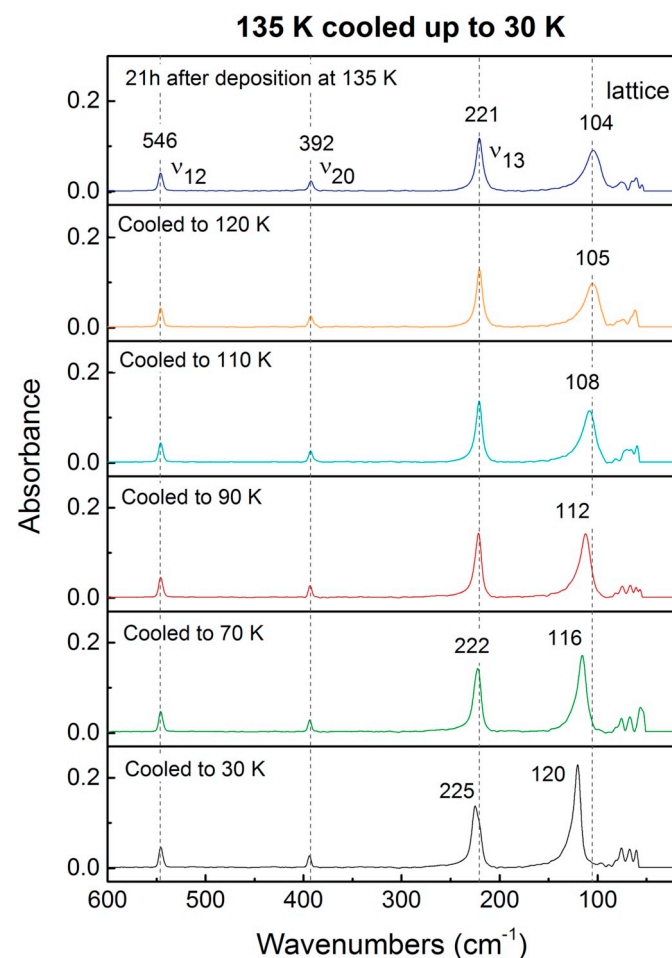

Fig. 11. Far-IR absorbance spectra of crystalline C_2H_5CN ice (3.77 μm thick film) deposited at 135 K and held at this temperature for 21 h after deposition, then cooled to 120 K, 110 K, 90 K, 70 K, and 30 K. Superimposed in the figures are the vibrational transitions and/or peak frequencies for the observed ice absorption bands.

Table 3

Observed infrared vibrational bands and frequencies of amorphous and crystalline propionitrile ice from the spectra obtained in this present study. The band assignments are based on previous published data.

	Amorphous (60 K) Observed infrared Frequencies (cm^{-1})[*]	Crystalline (135 K)[†] Observed infrared Frequencies (cm^{-1})[*]	Band assignment	Ref.[#]
Far-IR	112 s	105 s	Lattice	a
	223 m	221 m	ν_{13} C-C ≡ N planar bending	a, b, c
	388 s	392 s	ν_{20} C-C ≡ N out-of-plane bending	a, b, c
	547 m	546 m	ν_{12} C-C-C skeletal bending	a, b, c
Mid-IR	784 s	780 s[‡]	ν_{19} CH$_2$ rock	a, b, c
		764 vw[‡]		
	836 w	836 w	ν_{11} C−C sym. stretch	a, b, c
	1004 w	1014 w	ν_{10} CH$_3$ sym. rock	a, b, c
	1075 s	1074 s	ν_9 C−C non-sym. stretch	a, b, c
	1097 w	1095 w	—	
	1175 vw	1174 vw	ν_{18} CH$_3$ non-sym. rock	b
	1264 vw	1269 vw	ν_{17} CH$_2$ twist	a, b, c
	1318 m	1311 m	ν_8 CH$_2$ wag	a, b, c
	1384 m	1383 m	ν_7 CH$_3$ sym. bend	a, b, c
	1427 s	1435 s	ν_6 CH$_2$ deform.	a, b, c
	1462 vs	1458 vs[‡]	ν_5 and ν_{16} CH$_3$ non-sym. deform.	a, b, c
		1465 m[‡]		
	1647 vw	1656 vw	—	
	2246 vs	2245 vs[‡]	ν_4 C≡N stretch	a, b, c
		2260 w[‡]		
		2295 vw[‡]	—	
	2316 vw	2317 vw[‡]		
	2382 vw	2389 vw	$\nu_8 + \nu_9$	c
	—	2434 vw	$\nu_6 + \nu_{10}$	b
	—	2515 vw	$2\nu_{17}$	b
	2630 vw	2632 vw	$2\nu_8$	b
	2741 vw	2752 vw	$\nu_6 + \nu_8$	b
	2838 vw	2839 vw	ν_{15} CH$_2$ non-sym. stretch	b
	2891 m	2880 w[‡]	ν_2 CH$_3$ sym. stretch	a, b, c
		2893 m[‡]		
	2952 vs	2948 vs[‡]	ν_3 CH$_2$ sym. stretch	b, c
		2968 s[‡]		
	2992 vs	2990 vs	ν_1 and ν_{14} CH$_3$ non-sym. stretch	a, b, c
	3080 w	3080 w[‡]	$\nu_4 + \nu_{11}$	b
		3093 vw[‡]		
		3210 vw[‡]		
	3247 vw	3252 vw[‡]	$\nu_4 + \nu_{10}$	b
	S/N < 3	3328 vw	$\nu_4 + \nu_9$	c
Near-IR	S/N < 3	3359 vw	—	
	3507 w	3509 vw	—	
	3570 m	3536 vw[‡]	$\nu_4 + \nu_8$	c
		3559 vw[‡]		
	S/N < 3	3676 vw	—	
	S/N < 3	3728 vw	—	
	S/N < 3	3770 vw[‡]	—	
		3784 vw[‡]		
	S/N < 3	3827 vw	—	
	S/N < 3	3960 vw	—	
	4021 vw	4020 vw[‡]	—	
		4040 vw[‡]		
	4068 vw	4063 w[‡]	—	
		4084 vw[‡]	—	
		4100 vw[‡]	—	
	4220 vw	4227 w	—	
	4262 vw	4254 vw[‡]	—	
		4277 vw[‡]	—	
	4318 vw	4306 vw	—	
	4371 w	4354 vw[‡]	—	
		4375 w[‡]	—	
	4445 vw	4411 vw[‡]	—	
		4439 vw[‡]	—	
		4468 vw[‡]	—	
	5187 vw	5186 vw[‡]	—	
		5216 vw[‡]	—	
		5235 vw[‡]	—	
	5784 vw	5758 vw[‡]	—	
		5787 vw[‡]	—	
		5802 vw[‡]	—	
	5903 vw	5897 vw[‡]	—	
		5936 vw[‡]	—	

Table 3 (*continued*)

	Amorphous (60 K) Observed infrared Frequencies (cm^{-1})[*]	Crystalline (135 K)[†] Observed infrared Frequencies (cm^{-1})[*]	Band assignment	Ref.[#]
Near-IR	5982 *vw*	5981 *vw*	—	
	S/N < 3	6158 *vw*	—	
	S/N < 3	6501 *vw*	—	

— Unassigned frequencies.

[*] Intensities of band: vs very strong, s strong, m medium, w weak, vw very weak.

[†] Band frequencies observed for crystalline propionitrile at 135 K, 24 h after depositing.

[#] Band assignments are based on crystalline ice data in: (*a*) Dello Russo and Khanna (1996) and on liquid and gas phase data in: (*b*) Duncan and Janz (1955), (*c*) Klaboe and Grundnes (1968).

[‡] Two frequencies appear for the same vibrational assignment designate a band that is split into two. Features for which frequencies are not indicated, are below three times the noise level (S/N < 3) and therefore are not considered with sufficient confidence as absorption bands of C_2H_5CN ice.

is most noticeable in the low energy lattice modes of C_2H_5CN ice. In the Ennis et al. (2017) collisional cooling cell experiments, IR transmittance spectra from 50 cm^{-1} to 5000 cm^{-1} at 95 K, 110 K and 130 K were collected, with particular focus on the far-IR region to study the morphology of the icy aerosols, and to identify the crystalline phases. The investigators were unable to characterize a specific crystalline phase for C_2H_5CN. They reported that the lattice band of crystalline C_2H_5CN ice shifts towards lower energies with an increasing N_2 bath gas temperature (95 K to 132 K). Likewise, for their annealed crystalline C_2H_5CN, Moore et al. (2010) reported shifts in the position of the lattice band and also a change in band intensity when cooling the annealed ice from 110 K to 20 K.

After determining the crystalline temperature of C_2H_5CN ice, we also studied the behavior of crystalline propionitrile ice when cooling from 120 K to 30 K, after vapor deposition at 135 K (Fig. 11). We observe a band shift to higher frequencies by 1 cm^{-1} and 4 cm^{-1} in the ν_{13} C-C ≡ N in-plane bending mode at 221 cm^{-1}, when crystalline C_2H_5CN ice is cooled to 70 K and 30 K, respectively, but there is no shift observed at higher temperatures of 120 K, 110 K, and 90 K. However, the lattice mode at 104 cm^{-1} in the crystalline sample that was held for 24 h after deposition at 135 K, shifts to higher energies in all the studied cooling temperatures, and reaches a final shift of 16 cm^{-1} after the ice cooled to 30 K. On the contrary, the ν_{20} C-C ≡ N out-of-plane bending mode as well as the ν_{12} C-C-C skeletal bending mode do not undergo any band shifts.

3.2. Summary. Amorphous versus crystalline propionitrile ice

Table 3 lists the vibrational assignments for all infrared frequencies in the far-, mid- and near-IR observed in our experimental spectra of pure propionitrile ice in the amorphous and crystalline phases, deposited at 60 K and 135 K, respectively. Spectral peaks in the infrared spectra, which have signals rising above the 3σ noise level, have been considered with confidence as absorption bands of propionitrile ice, while features with a low signal-to-noise ratio (S/N < 3) have been disregarded.

The first detailed study of the far- and mid-IR spectra of propionitrile in gaseous and liquid phases was reported > 60 years ago (Duncan and Janz, 1955), in which the frequencies to the fundamental vibration modes of C_2H_5CN were assigned. The symmetry of propionitrile molecule was determined as Cs (or $C_{1\nu}$), describing that C_2H_5CN has one plane of symmetry σ as the only element of symmetry. The nine atoms of the molecule have collectively twenty-one degrees of vibrational freedom, divided into 13 of species *a′* and 8 of species *a″*, which are all infrared active (Duncan and Janz, 1955). Species *a′* and *a″* designate the symmetric and antisymmetric vibrations with respect to the plane of symmetry. We observed all the degrees of vibrational freedom listed in Duncan and Janz (1955) in our far-IR and mid-IR spectra of propionitrile ices. The IR spectral region between 6000 and 4500 cm^{-1} contains the first overtones of the CH stretching vibrations and no "mixed"

overtones involving $\nu(CH_2)$ and $\nu(CH_3)$ are of substantial intensity (Heise et al., 1981). Compared to the fundamental region (50–4500 cm^{-1}), the assignment of the bands in the region 6000 and 4500 cm^{-1} is still ambiguous because the infrared spectrum is still incompletely investigated for all propionitrile phases, and the assignment of the largely ternary combination bands in this high-frequencies region is not possible without further information.

Fig. 12 displays the far-IR spectra of propionitrile ice we have obtained for the amorphous phase (30 K to 90 K), intermediate phase (110 K to 130 K) and crystalline phase (≥135 K), while Figs. 13 and 14
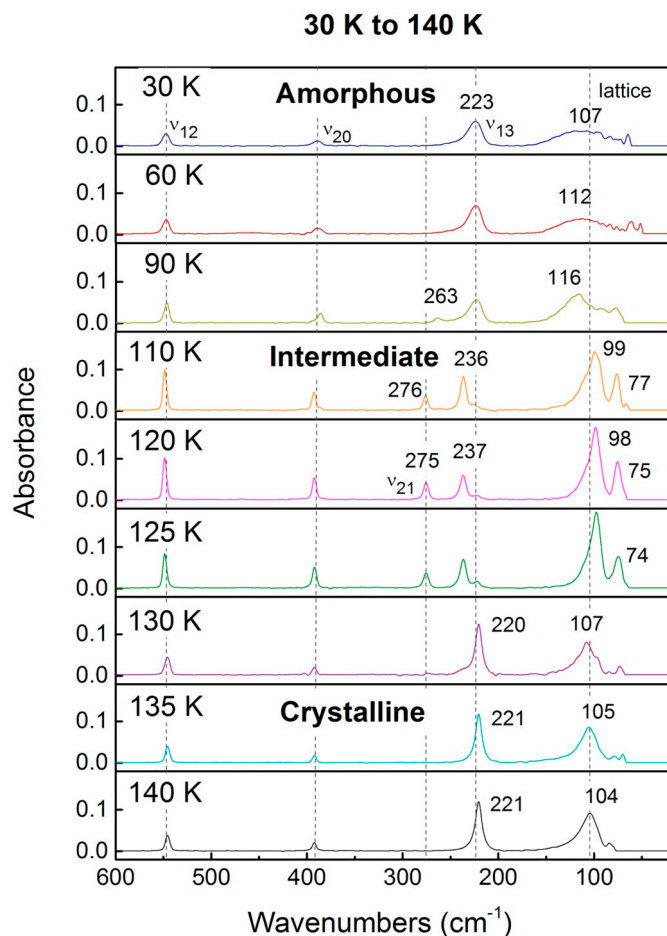

Fig. 12. Far-IR absorbance spectra of amorphous to crystalline C_2H_5CN ice (~4 μm thick film) obtained after depositing propionitrile vapors at temperatures from 30 K to 140 K and held several hours after deposition until no further spectral changes were observed. Superimposed in the figures are the peak frequencies for the observed ice absorption bands that are temperature-dependent.
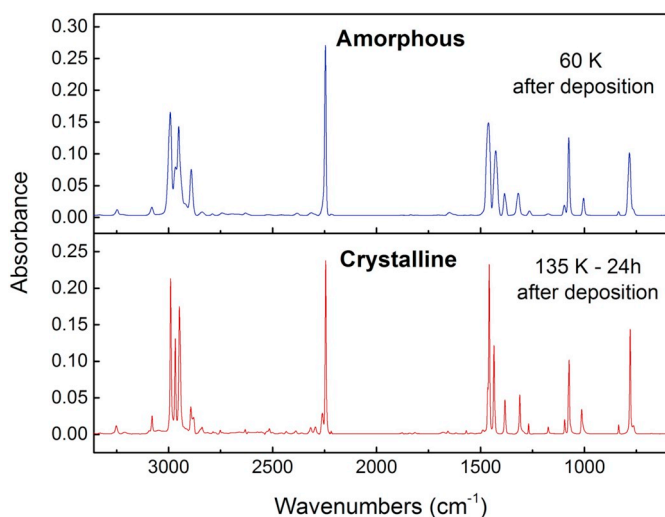
Fig. 13. Mid-IR absorbance spectra from 3350 to 600 cm^{-1} of amorphous and crystalline C_2H_5CN ice (3.95 μm and 3.85 μm thick films, respectively) obtained after depositing propionitrile vapors at 60 K and 135 K (the latter was held for 24 h after deposition).

show their corresponding mid-IR spectra (600–6600 cm^{-1}; 16.7–1.52 μm). For the ice film thicknesses used in this study, there were no C_2H_5CN ice absorption bands detected by our FTIR spectrometer at frequencies higher than 6550 cm^{-1}.

The refractive index (n_0) of propionitrile ice at each deposition temperature from 30 K to 135 K was determined from the resulting laser interference fringe patterns processed through a custom-developed IDL program (Anderson et al., 2018a). Table 4 lists the n_0 values obtained at 532 nm from the amorphous to crystalline phase. We have observed that the n_0 values differ slightly from one deposition temperature to another; however, there was no observed trend of these values as functions of deposition temperature. A more detailed study should be done to confirm this preliminary result by replicating the experiments at each deposition temperature to obtain a standard deviation on each value. Moore et al. (2010) reported n_0 values of 1.49 for annealed crystalline C_2H_5CN ice at 140 K and 1.26 for the amorphous ice at 30 K, using a 670 nm wavelength laser. Dello Russo (1994) assumed an n_0 value of 1.35 for the crystalline ice obtained after annealing at 140 K,
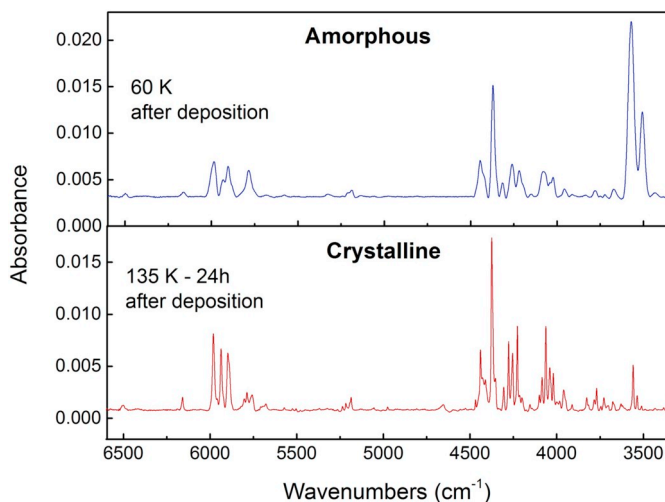

Fig. 14. Mid-IR absorbance spectra from 6600 to 3350 cm^{-1} of amorphous and crystalline C_2H_5CN ice (3.95 μm and 3.85 μm thick films, respectively) obtained after depositing propionitrile vapors at 60 K and 135 K (the latter was held for 24 h after deposition).

Table 4
Refractive index (n_0) of C_2H_5CN ice obtained at 532 nm from the amorphous to crystalline phase.

C_2H_5CN ice phase	Deposition temperature (K)	n_0
Amorphous	30	1.221 ± 0.018
	60	1.298 ± 0.003
	90	1.125 ± 0.042
Intermediate	110	1.035 ± 0.012
	120	1.318 ± 0.009
	125	1.305 ± 0.013
	130	1.383 ± 0.012
Crystalline	135	1.332 ± 0.012

which is close to the value of 1.33 that we have determined for the deposited crystalline C_2H_5CN ice at 135 K.

3.3. Study of propionitrile ices in the context of the chemically unidentified CIRS-observed haystack

Khanna (2005a) was the first to propose C_2H_5CN ice as the major contributor to Titan's Voyager 1 IRIS-observed 221 cm^{-1} spectral region, with minor contributions from both HC_3N and H_2O ices. Samuelson et al. (2007) then unambiguously ruled out pure C_2H_5CN ice as the chemical composition of the Haystack, although they reported that mixed ices may instead be responsible since mixing causes changes in both band shape and spectral position of an ice feature. de Kok et al. (2008) corroborated the Samuelson et al. (2007) findings that ruled out pure C_2H_5CN as the identity of the Haystack, reporting that the upper limit of C_2H_5CN gas is too low to form the Haystack via vapor condensation. The investigators concluded that instead, HCN ice plays an important role in the formation of the Haystack, by potentially mixing with other ices such as HC_3N, C_6H_6, or H_2O, or in the chemical alteration of HCN ice that would spectrally shift the 172 cm^{-1} HCN libration feature closer to 221 cm^{-1}. More recently, Ennis et al. (2017) proposed that future investigations should study composite ices containing C_2H_5CN/C_2H_2 or C_2H_5CN/C_6H_6. They pointed out that simulating heterogeneous aerosol ice particles, coupled with infrared spectroscopy, and using their collisional cooling cell is much more complicated than reproducing pure ice aerosols since they first need the optical constants (n and k) obtained from laboratory thin ice film data in order to model their crystalline-phase C_2H_5CN ice aerosols.

In this present study, we compared a simulated spectrum of Titan's stratosphere containing a C_2H_5CN ice cloud (derived from the laboratory spectrum of crystalline C_2H_5CN ice at 135 K -24 h post-deposition) to a CIRS-observed spectrum showing the Haystack (Fig. 15). The purpose of this short study is to illustrate the motivation behind our experimental work. Radiative transfer analyses are performed to match the ice cloud CIRS observations by using the computed optical constants of C_2H_5CN thin ice film. Synthetic simulated spectra are generated from the radiative transfer continuum model coupled with Mie scattering calculations for pure C_2H_5CN ice. Details on the radiative transfer analysis are provided in Anderson and Samuelson (2011), Anderson et al. (2018a) and references therein. Fig. 15 re-confirms the previously published results that propionitrile ice alone does not match the very intense and spectrally broad CIRS-observed Haystack emission feature. Although the ν_{13} C-C ≡ N bending vibration of our crystalline propionitrile ice peaks at the same frequency as that of the Haystack emission feature (at 221 cm^{-1}), it does not spectrally match the width of the Haystack band (even for large particle radii); but more importantly, the strong lattice mode of C_2H_5CN ice at 105 cm^{-1} is not present in the CIRS Titan limb spectra (shown in Fig. 15). Instead, it is the low-energy part of the far-IR coupled with the spectral width of the Haystack emission feature that suggests that the Haystack may result from co-condensation of mixed ices, which may not necessarily form via vapor condensation (Anderson et al., 2018b). Numerous co-condensed

ice clouds in Titan's stratosphere have been observed by CIRS, and are now thought to be more common than previously expected (Anderson et al., 2018b, and references therein). The next step is to obtain laboratory absorbance spectra of Haystack ice analogs, which involves measuring thin film transmittance spectra of mixed nitrile and hydrocarbon ices, with and without C_2H_5CN, under Titan mid to low stratospheric temperature conditions (70–155 K).

In Anderson et al. (2018a), we described the capabilities of our SPECTRAL ice chamber to simulate both layered and co-condensed ices observed by CIRS in Titan's stratosphere. In a preliminary attempt to identify the Haystack, we have initiated laboratory experiments of co-condensed ices containing relative degrees of various nitriles and hydrocarbons. We have tested one ternary mixture including propionitrile, that is presented in this manuscript. In application to the

Fig. 15. Cassini CIRS far-IR limb integration spectra of Titan recorded at a tangent height of 136 km in March 2005 at 85°N (orange curves). Twelve spectra are contained in the limb-integration averages. The black curves are synthetic spectra of our radiative transfer continuum model coupled with Mie scattering calculations for pure C_2H_5CN ice (upper panel) and a ternary ice mixture containing 16% HCN, 23% C_2H_5CN, and 61% C_6H_6 (lower panel). The optical constants were derived from our laboratory absorbance spectra of crystalline C_2H_5CN ice (24 h after vapor deposition at 135 K; upper black curve) and the ternary HCN-C_2H_5CN-C_6H_6 ice (mixed vapors deposited at 110 K; lower black curves), following the method described in Anderson et al. (2018a). The dash-dot black curve in the lower panel represents the ternary ice directly after vapor deposition, while the solid black curve shows the ternary ice after a 20 h delay. Superimposed in the upper panel are the vibrational transitions and peak frequencies for the observed C_2H_5CN ice absorption bands.

Haystack, we found a good opportunity to analyze a C_6H_6 – HCN - C_2H_5CN co-condensed ice, based on the estimated vertical distributions of organic vapors that condense in the altitudes of the CIRS-observed stratospheric clouds, including the Haystack, derived from their saturation vapor pressure curves (from CIRS analyses during the Cassini flyby in July 2015; see Anderson et al., 2018b and Figs. 1 and 9 therein).

In Fig. 15, we show one example of a ternary ice mixture containing 16% HCN, 23% C_2H_5CN, and 61% C_6H_6 (mixed vapors were deposited at 110 K). Once we computed the optical constants of this ternary co-condensed ice, we then ran again our forward radiative transfer continuum model coupled with Mie scattering calculations (using a log-normal particle size distribution- See details in Anderson et al., 2018a) and assumed a mean particle radius of 2 μm. The results are shown in the lower panel in Fig. 15 for both directly after vapor deposition and 20 h post-deposition. The continuum model includes opacity contributions from collision-induced absorption, Titan's aerosol, and Titan's 160 cm^{-1} co-condensed stratospheric ice cloud (model details are given in Anderson and Samuelson, 2011; Anderson et al., 2014, 2018b). The co-condensed ice displays a broad absorption band extending between 120 and 250 cm^{-1} as a result of mixing between the ν_{13} C-C ≡ N in-plane bending mode of C_2H_5CN and the lattice mode libration of HCN. Benzene also plays a non-negligible role in this ternary ice mixture. Although very preliminary, this result is encouraging as the best fit thus far obtained to match the width of the Haystack emission feature. However, there is certainly a mismatch in the spectral feature intensity between the Haystack and the ternary co-condensed ice mixture, and much more experimental work is needed to identify the chemical composition of the Haystack emission feature.

One of the reasons pure propionitrile ice was easily ruled out as the chemical identify of the Haystack emission feature was the absence of its intense lattice vibration band around 100 cm^{-1} in the CIRS-observed spectra. As shown in Fig. 15, when propionitrile is mixed with HCN and C_6H_6 and then co-deposited, the C_2H_5CN lattice band is dramatically weakened in the presence of the two other organic molecules. At 20 h post-deposition, the C_2H_5CN lattice vibration is significantly suppressed. This result demonstrates that the lattice mode of C_2H_5CN ice is not necessarily an impediment for the presence of C_2H_5CN ice in Titan's stratosphere, as long as it exists as part of a co-condensed ice. Both Samuelson et al. (2007) and Loison et al. (2015) briefly mentioned that the C_2H_5CN lattice mode could be strongly altered in the case of mixed ices, although the investigators did not perform any experimental work to support their speculations.

4. Conclusion

We have conducted a systematic and thorough study of propionitrile ice with the vapors directly deposited at temperatures between 30 K and 160 K. Such direct deposition studies (as opposed to annealing experiments) are almost nonexistent and are crucial to identify the chemical composition of Titan's CIRS-observed stratospheric ice clouds. We strongly emphasize that the standard annealing technique of ices from the amorphous to crystalline phase impedes the understanding and reproduction of Titan's observed stratospheric ices. We have experimentally observed that the far-infrared spectra of C_2H_5CN ice evolves significantly with the time held after deposition if a complete crystalline phase is not attained. We have also demonstrated that the quality of the ice crystalline structure formed in the laboratory (depending on the deposition temperature used in the experiments) is critical for the molecular identification since an incomplete crystalline phase can cause significant frequency shifts in the ice absorption bands, as well as variations in the shape, intensity, and width of the bands. As with previous investigators, we have also ruled out pure propionitrile ice as a possible chemical candidate for the CIRS-observed stratospheric Haystack ice cloud. We do, however, report the suppression of the lattice vibration of propionitrile ice when C_2H_5CN is co-condensed with
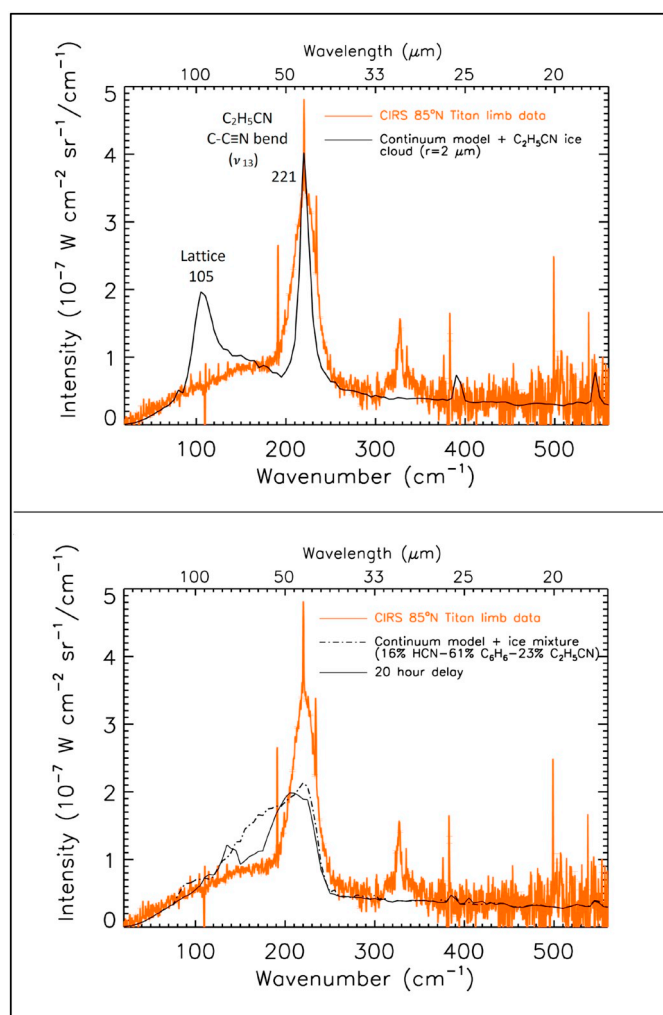
other organic ices. Further laboratory work is currently in progress to examine co-condensed organic ices with variable mixing ratios containing propionitrile and other organics, in an effort to discriminate between candidate ice mixtures as they may pertain to the chemical composition of Titan's Haystack.

Acknowledgments

D.N.-M acknowledges research funding support by the appointment to the NASA Postdoctoral Program at the NASA Goddard Space Flight Center, administered by the Universities Space Research Association (USRA) through contract with NASA. C.M.A. and R.E.S. acknowledge funding from both the Cassini Project and the Cassini Data Analysis Program under proposals 09-CDAP09-0020, 11-CDAPS11-0032, and 13-CDAPS13_2-0076 .

References

Anderson, C.M., Samuelson, R.E., 2011. Titan's aerosol and stratospheric ice opacities between 18 and 500 μm: vertical and spectral characteristics from Cassini CIRS. Icarus 212, 762–778.
Anderson, C.M., Samuelson, R.E., Achterberg, R.K., Barnes, J.W., Flasar, F.M., 2014. Subsidence-induced methane clouds in Titan's winter polar stratosphere and upper troposphere. Icarus 243, 129–138.
Anderson, C.M., Samuelson, R.E., Yung, Y.L., McLain, J.L., 2016. Solid-state photo-chemistry as a formation mechanism for Titan's stratospheric C4N2 ice clouds. Geophys. Res. Lett. 43, 3088–3094.
Anderson, C.M., Nna-Mvondo, D., Samuelson, R.E., McLain, J.L., Dworkin, J.P., 2018a. The SPECTRAL ice chamber: application to Titan's stratospheric ice clouds. Astrophys. J. 865, 62.
Anderson, C.M., Samuelson, R.E., Nna-Mvondo, D., 2018b. Organic ices in Titan's stratosphere. Space Sci. Rev. 214, 125.
Bertie, J.E., Whalley, E., 1967. Optical spectra of orientationally disordered crystals. II. Infrared spectrum of ice Ih and ice Ic from 360 to 50 cm^{-1}. J. Chem. Phys. 46, 1271–1284.
Coll, P., et al., 1999. Experimental laboratory simulation of Titan's atmosphere: aerosols and gas phase. Planetary and Space Science 47, 1331–1340.
Cordiner, M.A., et al., 2015. Ethyl cyanide on Titan: spectroscopic detection and mapping using Alma. The Astrophysical Journal Letters 800, L14.
Coustenis, A., Schmitt, B., Khanna, R.K., Trotta, F., 1999. Plausible condensates in Titan's stratosphere from voyager infrared spectra. Planetary and Space Science 47, 1305–1329.
Couturier-Tamburelli, I., Piétri, N., Gudipati, M.S., 2015. Simulation of Titan's atmospheric photochemistry. A&A 578, A111.
Couturier-Tamburelli, I., Toumi, A., Piétri, N., Chiavassa, T., 2018a. Behaviour of solid phase ethyl cyanide in simulated conditions of Titan. Icarus 300, 477–485.
Couturier-Tamburelli, I., Piétri, N., Le Letty, V., Chiavassa, T., Gudipati, M., 2018b. UV–Vis light-induced aging of titan's haze and ice. Astrophys. J. 852, 117.
Cravens, T.E., et al., 2006. Composition of Titan's ionosphere. Geophys. Res. Lett. 33.
Dello Russo, N., Khanna, R.K., 1996. Laboratory infrared spectroscopic studies of crystalline nitriles with relevance to outer planetary systems. Icarus 123, 366–395.
Dello Russo, N.P., 1994. Infrared Spectroscopic Studies of Condensed Nitriles With Relevance to Outer Planetary Systems. Ph.D. dissertation. University of Maryland College Park (174 pp).
Duncan, N.E., Janz, G.J., 1955. Molecular structure and vibrational spectra of ethyl cyanide. J. Chem. Phys. 23, 434–440.
Ennis, C., Auchettl, R., Ruzi, M., Robertson, E.G., 2017. Infrared characterisation of acetonitrile and propionitrile aerosols under Titan's atmospheric conditions. Phys. Chem. Chem. Phys. 19, 2915–2925.
Ennis, C., Auchettl, R., Appadoo, D.R.T., Robertson, E.G., 2018. The prediction of far-infrared spectra for planetary nitrile ices using periodic density functional theory with comparison to thin film experiments. Phys. Chem. Chem. Phys. 20, 23593–23605.
Frère, C., Raulin, F., Israel, G., Cabane, M., 1990. Microphysical modeling of titan's aerosols: application to the in situ analysis. Adv. Space Res. 10, 159–163.
Fujii, T., Arai, N., 1999. Analysis of N-containing hydrocarbon species produced by a CH$_4$/N$_2$ microwave discharge: simulation of Titan's atmosphere. Astrophys. J. 519, 858.
Hardin, A.H., Harvey, K.B., 1973. Temperature dependences of the ice I hydrogen bond spectral shifts—I: the vitreous to cubic ice I phase transformation. Spectrochim. Acta A: Mol. Spectrosc. 29, 1139–1151.
Heise, H.M., Winther, F., Lutz, H., 1981. The vibrational spectra of some isotopic species

of propionitrile. J. Mol. Spectrosc. 90, 531–571.
Hirschfeld, T., Mantz, A.W., 1976. Elimination of thin film infrared channel spectra in Fourier transform infrared spectroscopy. Appl. Spectrosc. 30, 552–553.
Hunklinger, S., 1982. Phonons in amorphous materials. J. Phys. Colloques. 43 (C9-461-C9-474).
Hurdis, E.C., Smyth, C.P., 1943. The structural effects of unsaturation and hyperconjugation in aldehydes, nitriles and chlorides as shown by their dipole moments in the vapor state. J. Am. Chem. Soc. 65, 89–96.
Jennings, D.E., et al., 2012a. First observation in the south of Titan's far-infrared 220 cm^{-1} cloud. The Astrophysical Journal Letters 761, L15.
Jennings, D.E., et al., 2012b. Seasonal disappearance of far-infrared haze in Titan's stratosphere. The Astrophysical Journal Letters 754, L3.
Jennings, D.E., et al., 2015. Evolution of the far-infrared cloud at Titan's south pole. The Astrophysical Journal Letters 804, L34.
Khanna, R., Allen, J., Masterson, C., Zhao, G., 1990. Thin-film infrared spectroscopic method for low-temperature vapor pressure measurements. J. Phys. Chem. 94, 440–442.
Khanna, R.K., 1995. Infrared spectroscopy of organics of planetological interest at low temperatures. Adv. Space Res. 16, 109–118.
Khanna, R.K., 2005a. Condensed species in Titan's atmosphere: identification of crystalline propionitrile (C$_2$H$_5$CN, CH$_3$CH$_2$CN) based on laboratory infrared data. Icarus 177, 116–121.
Khanna, R.K., 2005b. Condensed species in Titan's stratosphere: confirmation of crystalline cyanoacetylene (HC$_3$N) and evidence for crystalline acetylene (C$_2$H$_2$) on Titan. Icarus 178, 165–170.
Khanna, R.K., Ospina, M.J., Zhao, G., 1988. Infrared band extinctions and complex refractive indices of crystalline C$_2$H$_2$ and C$_4$H$_2$. Icarus 73, 527–535.
Klaboe, P., Grundnes, J., 1968. The vibrational spectra of propionitrile, 2-chloro and 2-bromo propionitrile. Spectrochim. Acta A: Mol. Spectrosc. 24, 1905–1916.
de Kok, R., et al., 2007. Characteristics of Titan's stratospheric aerosols and condensate clouds from Cassini CIRS far-infrared spectra. Icarus 191, 223–235.
de Kok, R., Irwin, P.G.J., Teanby, N.A., 2008. Condensation in Titan's stratosphere during polar winter. Icarus 197, 572–578.
Krasnopolsky, V.A., 2009. A photochemical model of Titan's atmosphere and ionosphere. Icarus 201, 226–256.
Loison, J.C., et al., 2015. The neutral photochemistry of nitriles, amines and imines in the atmosphere of Titan. Icarus 247, 218–247.
Magee, B.A., Waite, J.H., Mandt, K.E., Westlake, J., Bell, J., Gell, D.A., 2009. INMS-derived composition of Titan's upper atmosphere: analysis methods and model comparison. Planetary and Space Science 57, 1895–1916.
Marten, A., Hidayat, T., Biraud, Y., Moreno, R., 2002. New millimeter heterodyne observations of Titan: vertical distributions of nitriles HCN, HC$_3$N, CH$_3$CN, and the isotopic ratio ^{15}N/^{14}N in its atmosphere. Icarus 158, 532–544.
Masterson, C.M., Khanna, R.K., 1990. Absorption intensities and complex refractive indices of crystalline HCN, HC$_3$N, and C$_4$N$_2$ in the infrared region. Icarus 83, 83–92.
Moore, M.H., Hudson, R.L., 1992. Far-infrared spectral studies of phase changes in water ice induced by proton irradiation. Astrophys. J. 401, 353–360.
Moore, M.H., Hudson, R.L., 1994. Far-infrared spectra of cosmic-type pure and mixed ices. Astronomy and Astrophysics Supplement Series 103, 45–56.
Moore, M.H., Ferrante, R.F., Moore, W.J., Hudson, R., 2010. Infrared spectra and optical constants of nitrile ices relevant to Titan's atmosphere. Astrophys. J. Suppl. Ser. 191, 96.
Ospina, M., Zhao, G., Khanna, R.K., 1988. Absolute intensities and optical constants of crystalline C$_2$N$_2$ in the infrared region. Spectrochim. Acta A: Mol. Spectrosc. 44, 23–26.
Raulin, F., Owen, T., 2002. Organic chemistry and exobiology on Titan. Space Sci. Rev. 104, 377–394.
Sagan, C., Thompson, W.R., 1984. Production and condensation of organic gases in the atmosphere of Titan. Icarus 59, 133–161.
Samuelson, R.E., 1985. Clouds and aerosols of Titan's atmosphere. In: Rolfe, E. (Ed.), ESA Special Publication, Vol. ESA SP-241, pp. 99–107.
Samuelson, R.E., 1992. Infrared properties of Titan's clouds and aerosols. In: Kaldeich, B. (Ed.), Symposium on Titan. vol. 338.
Samuelson, R.E., Mayo, L.A., Knuckles, M.A., Khanna, R.J., 1997. C$_4$N$_2$ ice in Titan's north polar stratosphere. Planetary and Space Science 45, 941–948.
Samuelson, R.E., Smith, M.D., Achterberg, R.K., Pearl, J.C., 2007. Cassini CIRS update on stratospheric ices at Titan's winter pole. Icarus 189, 63–71.
Thompson, W.R., Henry, T.J., Schwartz, J.M., Khare, B.N., Sagan, C., 1991. Plasma discharge in N^2 + CH^4 at low pressures: experimental results and applications to Titan. Icarus 90, 57–73.
Vuitton, V., Yelle, R.V., Anicich, V.G., 2006. The nitrogen chemistry of Titan's upper atmosphere revealed. The Astrophysical Journal Letters 647, L175.
Vuitton, V., Yelle, R.V., McEwan, M.J., 2007. Ion chemistry and N-containing molecules in Titan's upper atmosphere. Icarus 191, 722–742.
Waite, J.H., et al., 2005. Ion neutral mass spectrometer results from the first flyby of Titan. Science 308, 982–986.